FY 2012 Engineering Research & Technology Report

Lawrence Livermore National Laboratory

A Message from
Monya Lane,
Associate Director for Engineering

THIS report summarizes key research, development, and technology advancements in Lawrence Livermore National Laboratory's Engineering Directorate for FY2012. These efforts exemplify Engineering's 60-year history of developing and applying the technology innovations needed for the Laboratory's national security missions, and embody Engineering's mission to "Create and apply engineering knowledge to advance national security."

Engineering's capability development strategy includes both fundamental research and technology development. Engineering research creates the competencies of the future where discovery-class groundwork is required. Our technology development (or reduction to practice) efforts enable many of the research breakthroughs across the Laboratory to translate from the world of basic research to the national security missions of the Laboratory. This portfolio approach produces new and advanced technological capabilities, and is a unique component of the value proposition of the Lawrence Livermore Laboratory. The balance of the report highlights this work in research and technology, organized into thematic technical areas: Computational Engineering, Engineering Information Systems, Micro/Nano-Devices and Structures, and Measurement Technologies. Our investments in these areas serve not only known programmatic requirements of today and tomorrow, but also anticipate the breakthrough engineering innovations that will be needed in the future.

Computational Engineering

Computational Engineering efforts focus on the research, development, and deployment of computational engineering technologies that provide the foundational capabilities to address most facets of Engineering's mission, ranging from fundamental advances to enable accurate modeling of full-scale DOE and DoD systems performing at their limits, to advances for treating photonic and microfluidic systems.

Project accomplishments in FY2012 included installing and testing a dedicated high-energy diffraction microscope and associated analysis code to enable in situ, three-dimensional x-ray characterization of polycrystalline materials; continuing improvements and extensions to core mechanical simulation engines such as DYNA3D and NIKE3D, and establishment of the Turbulence Analysis & Simulation Center (TASC) to enhance development efforts in fluid mechanics simulation; acquiring data and initial development of a model aimed at evaluating and reducing errors in predicting wind power; publishing preliminary findings and algorithm advancements related to improving our existing lattice-Boltzmann polymer code to enable fully turbulent, multiscale simulations of drag reduction; developing algorithms designed to reduce the computational cost of performing numerous parameter-dependent simulations; and applying and evaluating a previously developed Model Order Reduction technique to enhance performance of electromagnetic codes.

Engineering Information Systems

Knowledge discovery encompasses a wide variety of technologies with the goal of broadly generating new understanding or knowledge of relevant situations, thereby allowing anticipation or prediction of possible outcomes. With this understanding, a more comprehensive solution may be possible for problems as complex as the prediction of disease outbreaks or advance warning of terrorist threats.

Our FY2012 efforts were centered on first-stage development of a methodology and supporting framework for creating dynamic, mission-purposed Secure Virtual Network Enclaves; developing new, dynamic particle filters to be used in the creation of innovative computational learning algorithms that will enable the use of sophisticated predictive modeling techniques on modern streaming data sources; development and demonstration of large-scale optimization methods for electric power systems using high-performance computing platforms; examining how electric grid diagnostics and solar power forecasting could be used to advance energy related research opportunities; and creating data models as a first step toward establishing a foundation in energy systems informatics as a resource for LLNL projects, as well as for the greater energy utility user base.

Micro/Nano-Devices and Structures

Micro/nano-scale manufacturing encompasses technology efforts that fuel the commercial growth of microelectronics and sensors, while simultaneously customizing these technologies for unique, noncommercial applications that are mission-specific to the Laboratory and DOE. The Laboratory's R&D talent and unique fabrication facilities have enabled highly innovative and custom solutions to technology needs in Stockpile Stewardship, Homeland Security, and Intelligence.

FY2012 projects included ongoing work to develop inexpensive and portable approaches to molecular medical diagnostics for biosurveillance and force protection; research to develop plasmonic-based ultracompact lasers that can directly generate coherent optical fields at the nanometer scale; reviewing existing micro-mirror array technologies to determine theoretical performance limits and designing a new array of micro-mirrors with capabilities that approach the theoretical performance limits of general arrays; continued efforts to develop new, complementary embedded sensing capabilities for monitoring the stockpile: optic-fiber-based surface-enhanced Raman scattering and photo-acoustic spectroscopy; and additional work to continue developing microfluidic devices with integrated microchannels and membrane filters for separating and concentrating viruses.

Measurement Technologies

Measurement Technologies comprise activities in nondestructive characterization, metrology, sensor systems, and ultrafast technologies for advanced diagnostics. The advances in this area are essential for the future experimental needs in Inertial Confinement Fusion, High-Energy-Density Physics, Weapons, and Department of Homeland Security programs.

Our FY2012 projects consisted of work to establish a protocol for aligning x-ray computed tomography (CT) systems, combining high-precision radiography phantoms and software alignment algorithms; characterizing the system performance of a newly procured nanometer-scale, three-dimensional x-ray CT system that will benefit multiple programmatic efforts; continued efforts to gain a fundamental understanding of the acceleration gradients in Dense Plasma Focus (DPF) Z-pinch plasmas in order to examine how these plasmas can be systematically exploited for accelerator applications; and additional development toward a new class of ultrafast, sensitive gamma, neutron, and proton detectors that leverage recent advances in the development of high-bandwidth x-ray-to-optical converters and high-bandwidth optical recording technologies.

Micro/Nano-Devices and Structures

Measurement Technologies

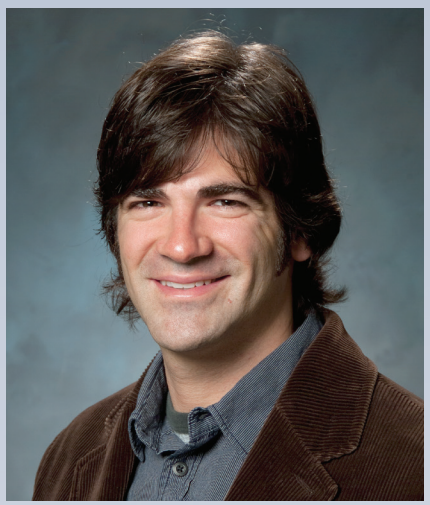

Joel V. Bernier

In Situ Observation and Characterization of Phase Transformations and Twinning

Project Overview

We will develop a fully three-dimensional x-ray characterization technique for polycrystalline materials. Referred to as high-energy diffraction microscopy (HEDM), this technique is essentially a variant of the classical rotation method adapted to high-energy (≤35 keV) synchrotron sources and large, fast panel detectors [1]. Our project involves developing this capability at the Advanced Photon Source (APS) beamline 1-ID, which includes hardware, methodologies, and analysis software.

Project Goals

This new HEDM technique will be capable of:

- Identifying the orientations (≤ 0.05°) and centers of mass (≤ 5 μm) of individual embedded grains in polycrystals containing up to 1000 grains.
- Providing average strain/stress tensors for each grain with strain resolution of at least 0.0001.
- Accommodating quasistatic thermomechanical loading in situ up to 100 GPa and 1000 K using a diamond anvil cell (DAC).

The exit strategy involves application of HEDM to material systems of critical importance to the Laboratory, as well as performing measurements related to strength and damage in support of projects for the Department of Defense. Ultimately, there will be a dedicated HEDM instrument at APS 1-ID that is available to the general synchrotron user community.

Relevance to LLNL Mission

This work contributes directly to LLNL's technical proficiency outlined under the Science, Technology, and Engineering pillars, encompassing Materials on Demand and

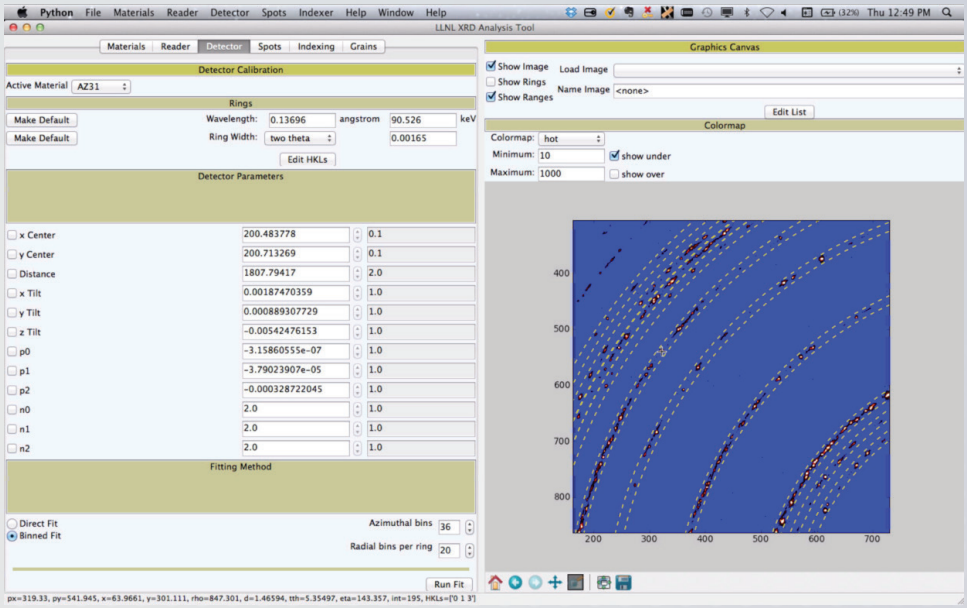

Figure 1. Screenshot of the heXRD program, showing the detector interface and a composite HEDM image on the graphics canvas. The detector panel contains the interface to calibration tools as well as for selecting the active material used for overlays. The graphics canvas shows overlays for a subset of reciprocal lattice vector types for an AZ31 magnesium alloy superimposed on a composite image. The bright spots are Bragg reflections from individual grains.

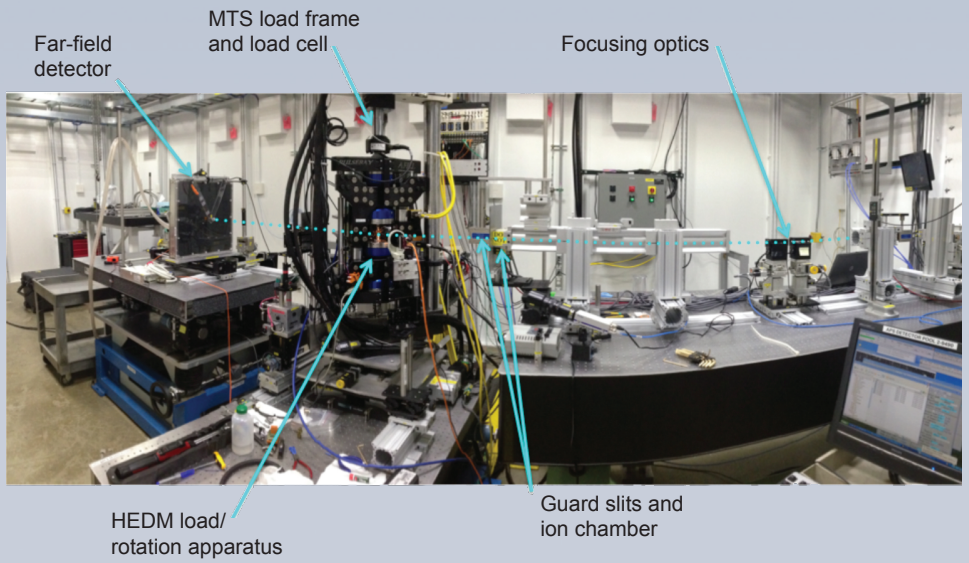

Figure 2. HEDM instrument implemented at APS 1-ID-E.

Measurement Science and Technology. High-fidelity materials models also comprise a critical piece of the multiphysics simulation codes used at LLNL in support of Stockpile Stewardship Science goals; the data from HEDM measurements provide an invaluable touchstone for model formulation and validation.

Other fields benefiting from an enhanced understanding of twinning and phase transformations include geophysics (e.g., paleopiezometry and planetary interiors) and industrial deformation processing (e.g., forming of low-symmetry metals like magnesium). Direct observations of these phenomena in situ, at the crystal scale, represent first-of-kind, discovery-class science.

FY2012 Accomplishments and Results

The open-source analysis code heXRD (LLNL-CODE- 529294) was publicly released in FY2012 (see Figure 1). It has already gained ongoing development support and a nascent user community at both APS and the Cornell High Energy Synchrotron Source (CHESS). The heXRD project represents a significant contribution to the synchrotron user facility and a major step toward moving HEDM ahead as a rapid-throughput characterization tool suitable for industry.

A dedicated HEDM instrument, shown in Figure 2, was installed and tested at APS 1-ID-E in the fourth quarter. The device was developed and fabricated in collaboration with the Air Force Research Laboratory under a Partner User Proposal at the APS. The team will participate in the continued development of the instrument under work-for-others funding in FY2013 and FY2014.

Some of the salient scientific highlights obtained over the course of this project include:

- Identified that the $\alpha \rightarrow \varepsilon$ phase transition in iron obeys a Burgers relation at quasistatic loading rates and ambient temperature (see Figure 3). Results indicate very good agreement with the Burgers pathway, with preferred variant selection (higher intensity)

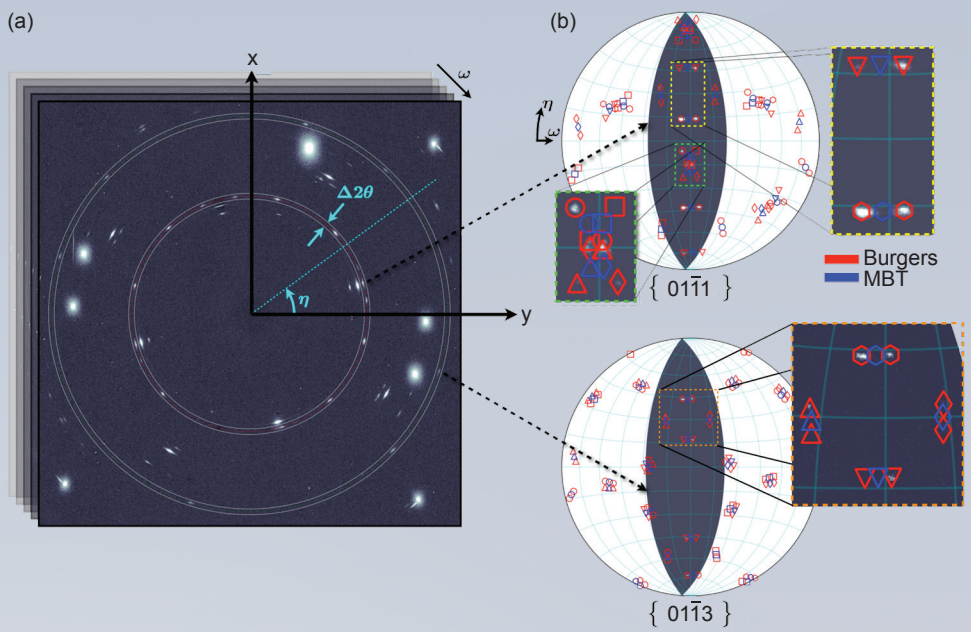

Figure 3. Primary result from the high-pressure phase transition study in iron. (a) Oscillation image stacks recorded at pressure contain the diffraction spots from α-iron, ε-iron and diamond. (b) The regions within Δ2θ of the Debye rings are collapsed on each image and binned over the stack to generate η-ω "pole figures," which show the expected signal locations associated with the Burgers and MBT pathways (red and blue glyphs, respectively).

evident under the influence of the nonhydrostatic stress in the diamond anvil cell. This result answers a long-standing question in materials science as to the nature of the mechanism that underlies this widely studied phase transition.

- Positively correlated ε-phase variant selection with applied deviatoric stress in iron.
- Identified regions of mutually exclusive ε-phase variants at the scale of ~1 μm in iron.
- Identified the absence of a fixed orientation relationship in the α → γ phase transition in iron.
- Identified two orientation relationships for the α → ω phase transition in zirconium.

Related References

1. Bernier, J. V., N. R. Barton, U. Lienert, and M. P. Miller, "Far-Field High-Energy Diffraction Microscopy: A Tool for Intergranular Orientation and Strain Analysis," *J. Strain Anal. Eng.*, **46**(7), 527–547, 2011.
2. Edmiston, J. K., N. R. Barton, J. V. Bernier, G. C. Johnson, and D. J. Steigmann, "Precision of Lattice Strain and Orientation Measurements Using High-Energy Monochromatic X-Ray Diffraction," *J. Appl. Cryst.*, 44, 299–312, 2011.
3. Edmiston, J. K., J. Bernier, N. Barton, G. Johnson, D. Steigmann, "Lattice Refinement Strategies," *Acta Cryst. A* **A68**(2):181–187, 2012.
4. S. F. Li, J. Lind, C. M. Hefferan, R. Pokharel, U. Lienert, A. D. Rollett, R. M. Suter, "Three Dimensional Plastic Response in Polycrystalline Copper Via Near-Field High Energy X-ray Diffraction Microscopy," *J. Appl. Cryst.* **45**(6):1098–1108, 2012.
5. Barton, N. R. and J. V. Bernier, "A Method for Sub-grain Orientation and Lattice Strain Distribution Determination," *J. Appl. Cryst.* 45, 1145–1155, 2012.
6. Li, S. F. and R. M. Suter, "Adaptive Reconstruction Method for Three-Dimensional Orientation Imaging," *J. Appl. Cryst.*, accepted for publication (2013).

Engineering Simulation

Bob Ferencz

Project Overview

Institutional funding contributes to the continued development and use of key simulation tools to support Laboratory programs and external sponsors. In particular, a set of in-house codes for simulating the highly nonlinear response of mechanical assemblies and structures provides a capability to assess performance margins under extreme environments. To grow a complementary capability for fluid systems, we are leveraging DOE investments in computational fluid dynamics tools at Stanford University. Our code portfolio, along with the expert personnel that sustain it, is the foundation for the delivery of key assessments by dozens of sophisticated users.

Project Goals

Our goal is to sustain operation and continuous improvement of simulation capabilities founded upon continuum and structural mechanics. In the context of simulation tools, "operation" encompasses feature addition, maintenance, platform ports, and user support and consultation. It is essential to enabling an overall simulation workflow. Thus, in addition to the core simulation engines DYNA3D [1] and NIKE3D [2], we support tools that permit analysts to interrogate and interpret their results. Major simulation technology advances are typically funded separately through LDRD research grants, program investments, or outside sponsorship. The large-scale parallel computing counterparts to DYNA3D and NIKE3D—ParaDyn and Diablo—are supported under the NNSA's Advanced Simulation and Computing Program.

Relevance to LLNL Mission

Engineering analysts supporting a variety of programs require advanced modeling functionalities and technical consultation to meet their mission deliverables. In addition to our NNSA-sponsored efforts, programs and projects involve the Laboratory's collaborations with the Missile Defense Agency, Naval Surface Warfare Center,

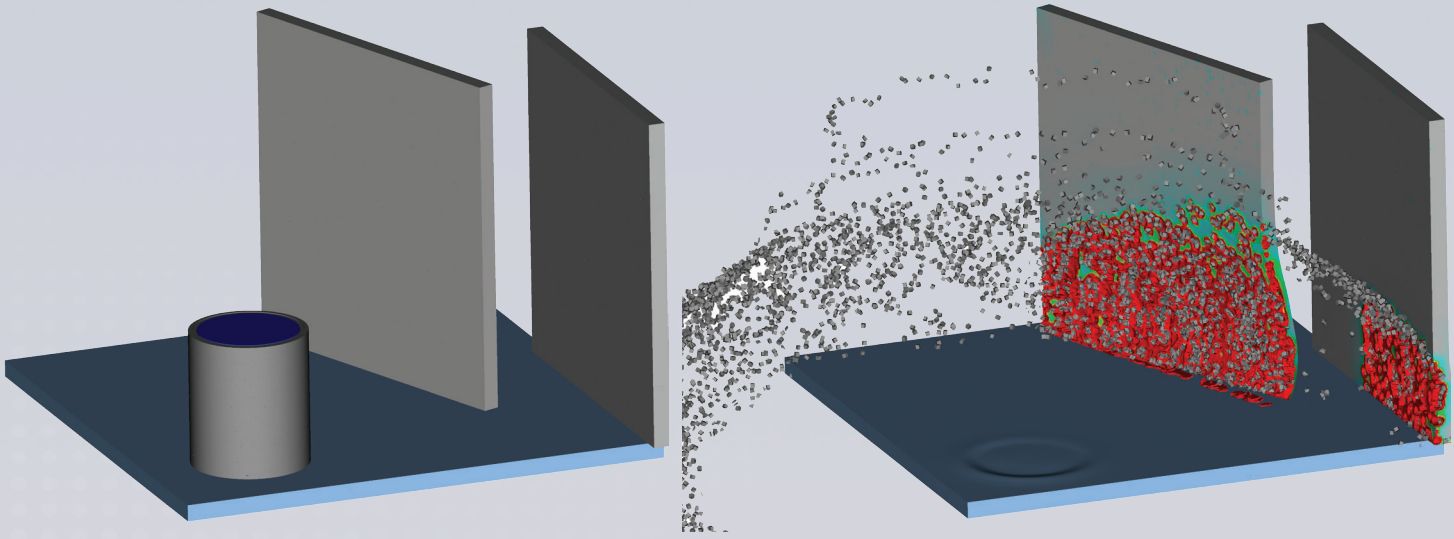

Figure 1. A simulation of an explosion inside a cylinder showing the initial setup (left) and the global pattern of shrapnel (right) striking two witness plates.

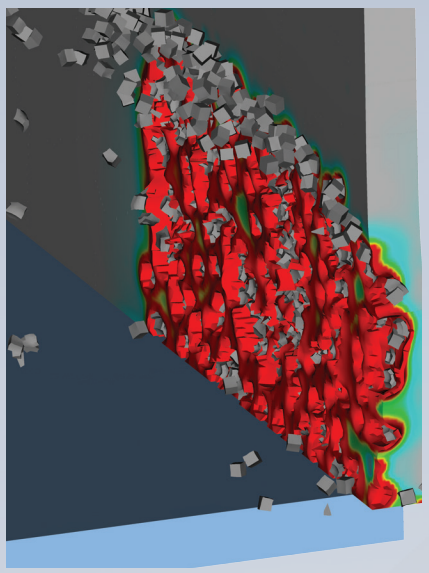

Figure 2. Details of shrapnel from cylinder impacting a witness plate and the resulting regions of high damage.

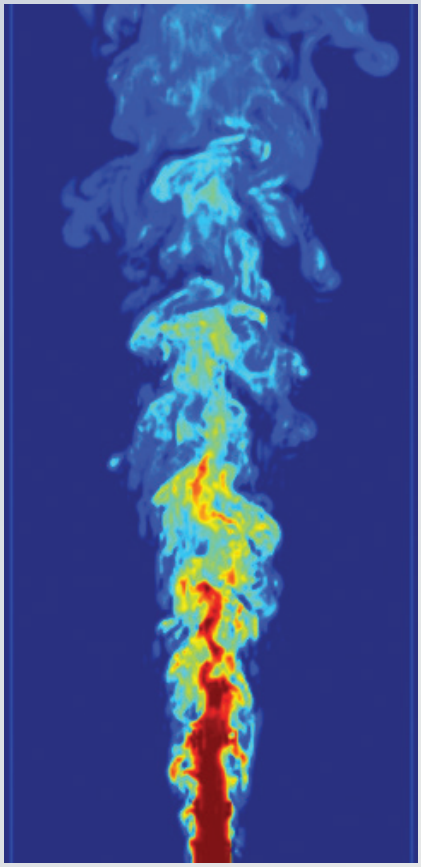

Figure 3. Mixing of a 3D round, turbulent jet at high Schmidt-number mixing (Sc = 1024) illustrated with a passive scalar concentration field.

US Army Research Laboratory, and Department of Homeland Security. Some examples of programmatic applications may be found on-line [3].

FY2012 Accomplishments and Results

DYNA3D and ParaDyn were used for millions of CPU hours in FY2012, typically to examine the rapid transient response of structures to abrupt loadings. Figure 1 illustrates an example of a cylinder packed with energetic material that explodes to create shrapnel. Such simulations are used to assess both the global distribution of debris, and as shown in Figure 2, the local details of interaction and damage. Development efforts in DYNA3D included incorporating an initial implementation of the eXtended Finite Element Method (X-FEM) for shell element fracture as prototyped by an academic collaborator. Our database utilities were enhanced to provide more flexibility in representing auxiliary results such as contact pressure and to increase performance for very large databases. Analysts continue the progression toward running finer meshes (spatial resolution) and writing results more frequently (temporal resolution).

While Engineering has invested in solid mechanics code development for decades, the programmatic needs for fluid mechanics simulation have typically been handled through commercial codes. Seeing a need for greater high-performance computing for fluids, the Turbulence Analysis & Simulation Center (TASC) was created to leverage third-party codes that can run on the large parallel computing resources at LLNL. Due to past and ongoing collaborations with Stanford University researchers, several Stanford codes were obtained and ported to LLNL platforms. Stanford codes such as CharlesX represent state-of-the-art capabilities. Another code in the TASC portfolio, developed by engineer Greg Burton, includes an advanced turbulence model (nLES) for incompressible turbulent flow, which can be used to explore mixing/dispersion problems, as shown in Figure 3.

FY2013 Proposed Work

In FY2013, general technical support for structural analysis users, the addition of user-requested capabilities, and software quality assurance practices will continue. To complement our advanced simulation engines, we will continue to enhance auxiliary tools required to interrogate structural analysis output. Targeted efforts in computational fluid dynamics tools suitable for engineering analysis will likely also continue.

References

1. E. Zywicz and J.I. Lin, “DYNA3D: A Nonlinear, Explicit, Three-Dimensional Finite Element Code for Solid and Structural Mechanics: Version 12.1,” Lawrence Livermore National Laboratory, LLNL-SM-599533, October 2012.
2. M.A. Puso, “NIKE3D: A Nonlinear, Implicit, Three-Dimensional Finite Element Code for Solid and Structural Mechanics,” Lawrence Livermore National Laboratory, LLNL-SM-563704, June 2012.
3. “Engineered Solutions through Simulation Insights,” *Science & Technology Review*, Lawrence Livermore National Laboratory, UCRL-TR-52000-12-9, September 2012. https://str.llnl.gov/Sep12/ferencz.html
4. Turbulence Analysis and Simulation Center, LLNL-WEB-643214. https://tasc.llnl.gov/

Reducing Uncertainties in Wind Power Forecasting

Wayne Miller

Project Overview

The current U.S. goal is to achieve 20% wind power by 2030. Accurate forecasts of wind power are needed by utilities as they add more renewable energy onto the power grid. Renewables such as wind and solar present a significant challenge for grid integration as they only produce power when the wind blows and the sun shines, which means they have a random and unpredictable aspect (Figure 1). In contrast, utility markets have relied on power production from carbon and nuclear sources, which are much easier to match against demand. Thus, as more renewable energy is deployed, accurate forecasts of their power are needed to anticipate and balance all energy production against demand.

Errors in wind power forecasts come from several sources. Foremost is the challenge of weather prediction. We have imperfect knowledge of the initial conditions and physics of the weather, and therefore many assumptions must be made to generate a single forecast. As a result, ensembles of many forecasts are used to provide statistics and error bounds. The numerical solution of the forecasts also introduces error from round-off and discretization. Ultimately we need accurate forecasts of the winds in and around turbines, which is not typically resolved today. Finally, we must consider the turbine response. Modern turbines can produce up to 5 MW each and have a rotor diameter exceeding 100 m—and the trend is for larger machines in the future. With turbines of that size, the wind will vary substantially

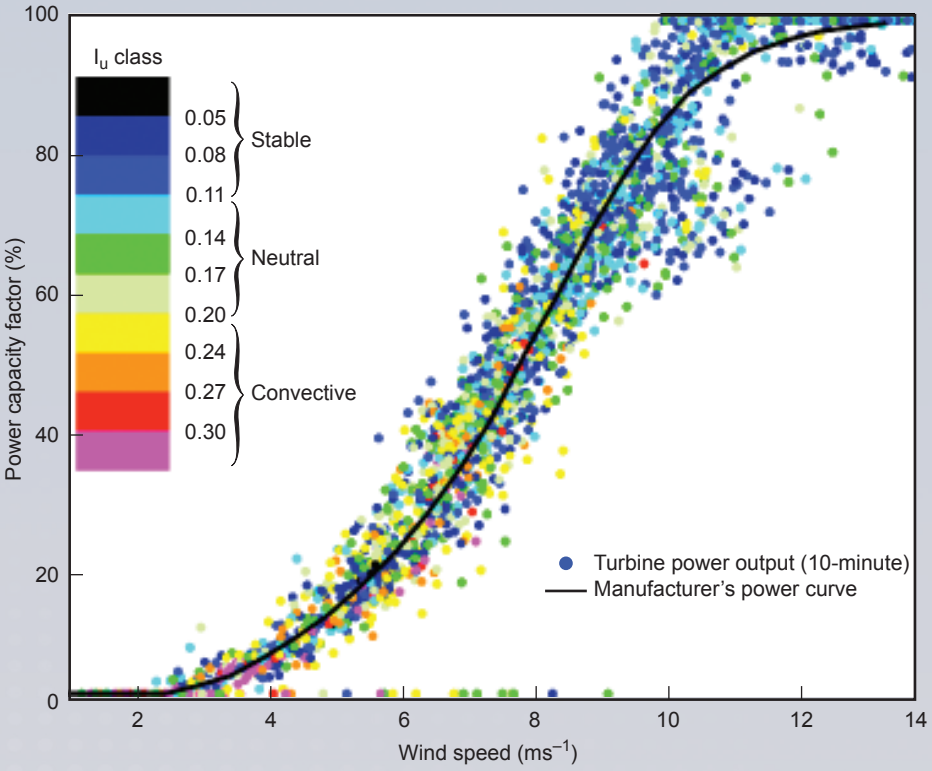

Figure 1. Expected turbine power output (black curve) may be very different from actual power production (dots) due to complex atmospheric winds.

across the rotor disc due to turbulence, shear, and other complications of the atmospheric boundary layer in which they operate. The result is that we cannot now accurately predict how much power a turbine will produce with an average wind speed. Rather we must add the complications into the equation to get a more accurate, but also more complex, understanding of the turbine output.

We want to transfer our findings into the hands of industry to reduce the costs of power and allow more renewables into the mix. Industry does not have the resources that we have at LLNL, and so we include deliverables that are useful to industry. In particular we focus on reduced-order models of wind forecast accuracy and turbine power production that will be trained by our extensive data, but which will have modest requirements to use. Imagine, for example, a smartphone app trained by millions of CPU hours.

Project Goals

The purpose of this project is to evaluate and reduce the sources of error in predicting wind power. Our overall goals are to:

- Formulate and execute a process for uncertainty quantification of wind power.
- Identify and quantify sources of error in wind forecasts.
- Identify and quantify sources of error in turbine power forecasts.
- Improve the state of the art in forecasting simulations for wind power.
- Identify and demonstrate best practices for wind power forecasting.
- Validate wind power forecasts with a rigorous field data campaign.
- Create a reduced-order model of turbine performance.

Relevance to LLNL Mission

The challenge of renewable power intermittency and predictability at large scales has been recognized at the Federal level as a topic of national importance with significant technical obstacles. Success in meeting this challenge is also in line with the LLNL roadmap relating to energy security and climate change, and research activities in renewable energy and utility power analysis.

Figure 2. Field data acquisition is a critical aspect of the research for validation of forecasts. We are collecting atmospheric data and turbine performance data (Site 300 shown).

FY2012 Accomplishments and Results

During this past year, we acquired field data at two locations, Site 300 and an adjacent wind farm (Figure 2). At Site 300, the existing meteorological tower and a mobile LIDAR were used. At the wind farm, we used a mobile LIDAR and the wind farm's SCADA data to provide turbine power output as a function of inflow wind.

We tested forecast ensembles using the WRF code with varying physics packages and parameters. We ran a large ensemble forecast over the wind farm. The variations identified forecast error sensitivity to initial conditions and physics assumptions (Figure 3).

We began developing a reduced-order model for turbine power that improves the standard power curves. We correlated inflow winds to the measured turbine power output.

We also prototyped the UQ process for evaluating ensemble errors on turbine power output and contracted with the University of Wyoming to couple WRF with the rotor CFD code HELIOS. We can now simulate realistic atmospheric winds acting on a turbine to get loads and power.

FY2013 Proposed Work

During the upcoming year, we plan to:

- Perform extensive WRF ensemble forecasting and error analysis.
- Extract turbulence metrics from LIDAR data.
- Enhance the CGWIND code for high-resolution complex terrain.
- Further the development of the turbine power model.

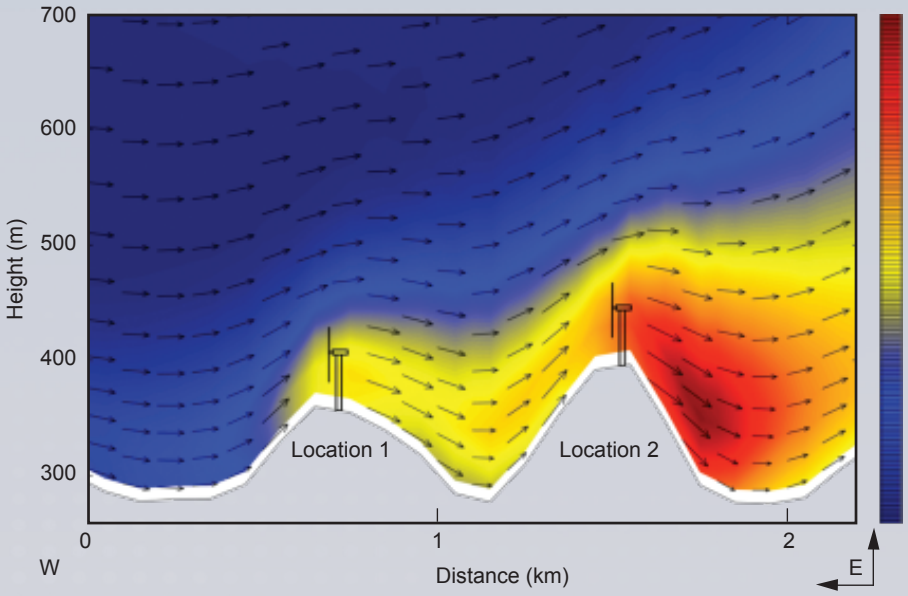

Figure 3. Resolved wind forecasts in complex terrain are a challenge for power prediction (Turbulent kinetic energy cross-section, valid 20 June 2010, 00 UTC).

Figure 4. Ensemble forecasts of turbine power output show sensitivity to modeling assumptions. Black lines are individual forecast perturbations. The red line is actual power output for validation.

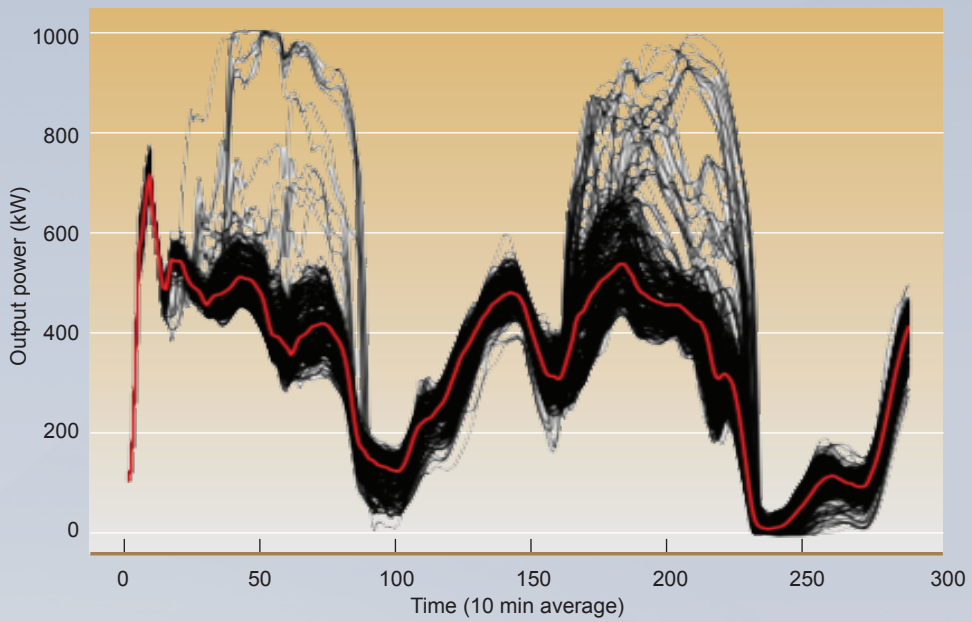

Related References

1. *20% Wind Energy by 2030: Increasing Wind Energy's Contribution to U.S. Electrical Supply*, DOE/GO-102008-2567, July 2008.
2. Wharton, S. and J. Lundquist, "Atmospheric stability affects wind turbine power collection," *Environmental Research Letters* 7, 014005, 2012.
3. Mirocha, J., G. Kirkil, E. Bou-Zeid, F. Katopodes-Chow, and B. Kosovic, "Transition and Equilibration of Neutral Atmospheric Boundary Layer Flow in One-Way Nested Large-Eddy Simulations Using the Weather Research and Forecasting Model," *Monthly Weather Review*, doi:10.1175/MWR-D-11-00263.1, in press.

Multiscale Polymer Flows and Drag Reduction

Todd H. Weisgraber

Project Overview

Suspensions and polymer solutions exhibit a variety of complex physical phenomena and have applications across multiple disciplines, including such disparate subjects as blood flow and materials processing. In particular, drag reduction in bounded turbulent flows caused by the addition of long-chain polymers is a well-established phenomenon. However, despite decades of research, there is still a lack of understanding of the fundamental mechanisms. We believe that a complete description must incorporate wall roughness, a coarse-grained molecular representation of the polymer, and hydrodynamic fluctuations at the polymer length scale. We are developing new algorithms, including an unconditionally stable, fluctuating lattice-Boltzmann solver coupled with molecular dynamics (MD), to enable fully turbulent, multiscale simulations of drag reduction.

Project Goals

Our ultimate goal is to perform a series of large-scale simulations of dilute polymer solutions in turbulent flows with a detailed model of the polymer chains and the hydrodynamic interactions. To resolve the relevant scales, we are incorporating three improvements to our existing lattice-Boltzmann (LB) polymer code: enhanced numerical stability, accurate hydrodynamic fluctuations, and integration of the solver with an adaptive mesh refinement (AMR) framework.

Relevance to LLNL Mission

Our research aligns with LLNL's focus on high-performance computing and simulation. Specifically, we seek to address fundamental scientific questions in hydrodynamics. The role of rough boundaries in turbulent transition and drag reduction is also relevant to Global Security efforts in heavy vehicle aerodynamics and wind energy.

FY2012 Accomplishments and Results

This third year emphasized applying our AMR code to large-scale simulations of turbulent transition in channels induced by a realistic representation of wall roughness. We hypothesized that the length scales associated with roughness amplitudes are important in understanding transition, and we have demonstrated via direct simulation that an instability that leads to turbulence is generated by finite amplitude roughness. This year we published our preliminary findings in addition to our AMR algorithm advancements.

Our approach to lattice-Boltzmann AMR is based on fully conservative interpolation and streaming algorithms to advance the solution at coarse–fine grid interfaces. This innovation produced lower errors than in previous lattice-Boltzmann mesh refinement efforts. Figure 1 shows a snapshot of the flow field for the Taylor-Green vortex benchmark problem. An initial array of counter-rotating vortices becomes unstable and transitions to a turbulent flow, producing a range of small scales through vortex stretching. Without an external source to maintain it, the flow eventually decays. We ran simulations using single and two-level AMR grids and computed the kinetic energy

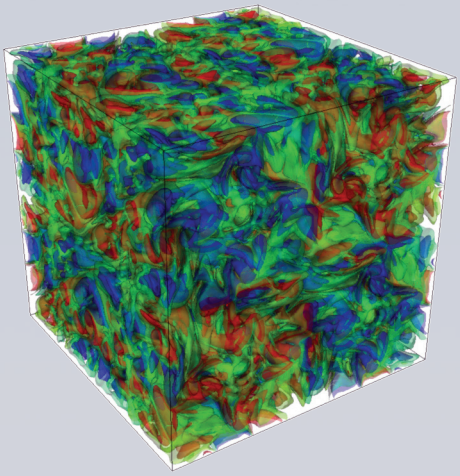

Figure 1. Turbulent flow initiated by a three-dimensional Taylor-Green array of counter-rotating vortices. The colors denote isosurfaces of the vertical component of vorticity.

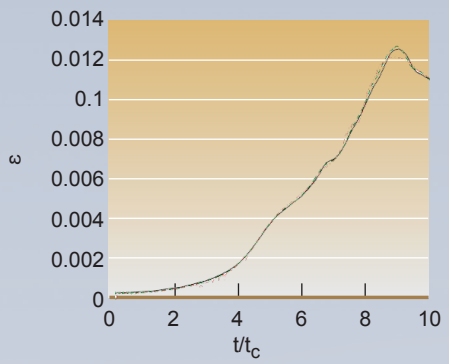

Figure 2. Evolution of the Taylor-Green turbulent energy dissipation: pseudo-spectral method (solid black) [2], lattice-Boltzmann single grid (dashed green), and lattice-Boltzmann AMR (dash-dot red).

dissipation, which has a well-defined peak for this flow. In Figure 2 we compare the results of our calculations with those from a pseudo-spectral method simulation at a much higher resolution. Both the single grid and AMR produced dissipation curves in excellent agreement with the spectral method.

One advantage of lattice-Boltzmann is a simplified implementation of boundary conditions. As a demonstration to our Global Security collaborators, we simulated the flow past an Ahmed body (Figure 3), an industry standard geometry used to study the relevant flow phenomena for heavy vehicles. There is some evidence that lattice-Boltzmann more accurately captures the dynamics of these flows than conventional fluid solvers and, therefore, our code could be a useful tool for improving the energy efficiency of the next generation of heavy vehicles.

Project Summary

We developed a conservative AMR methodology for the lattice-Boltzmann method with our collaborator at LBL, Phillip Colella, and demonstrated that our approach has a higher order of convergence and less numerical error than established methods. Using this capability, we performed preliminary direct simulations of channel flow instability solely due to perturbations initiated by three-dimensional distributed roughness elements. Results indicate the roughness amplifies disturbances in the form of streamwise vortices, which is consistent with some experimental observations.

Related References:

1. Rohde M., D. Kandhai, J.J. Derksen, H.E.A. van den Akker, "A generic, mass conservative local grid refinement technique for lattice-Boltzmann schemes," *Int. J. Numer. Methods Fluids* **51**(4):439–46, 2006.
2. van Rees, W.M., A. Leonard, D. I. Pullin, P. Koumoutsakos, "A comparison of vortex and pseudo-spectral methods for the simulation of periodic vortical flows at high Reynolds numbers," *J. Comput. Phys.* 230, 2794–2805, 2011.
3. Weisgraber, T.H. and B. J. Alder, "Computer experiments on the onset of turbulence," *28th Rarefied Gas Dynamics Conference, AIP Conference Proceedings 1501*, 2012.
4. Guzik, S.M., T. H. Weisgraber, P. Colella, and B. J. Alder, "Interpolation methods and the accuracy of lattice-Boltzmann mesh refinement, submitted to *J. Comp. Phys.*

Figure 3. Streamlines and wake vortex structure for flow past an Ahmed body computed with lattice-Boltzmann AMR.

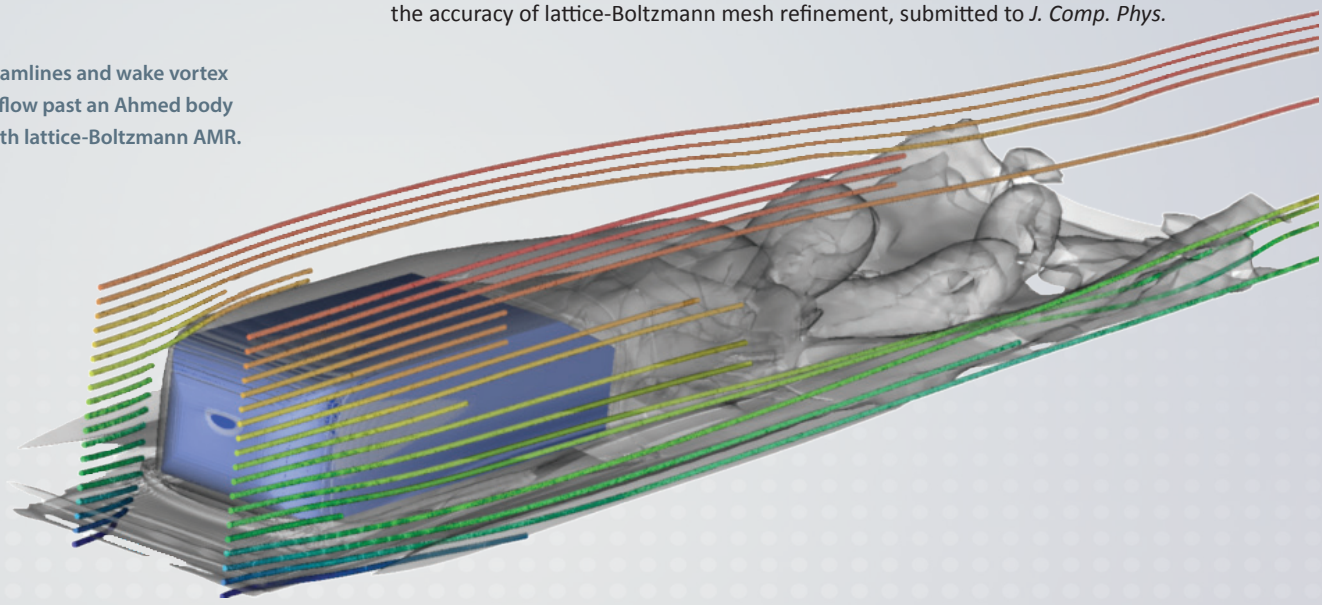

Automatic Complexity Reduction with Application to Electromagnetic Effects Simulation

Dan White

Project Overview

Documented experimental evidence demonstrates that an electromagnetic wave of modest power (tens of watts/meter^2) incident upon an electronic circuit can temporarily shut down the electronic circuit. This is what we mean by "electromagnetic effect," and prototype hardware systems have been developed to exploit it. But there is no explanation for why some circuits are affected and others are not. Also, the prototype systems perform better in a laboratory setting than they did in the field, and there is no explanation why performance is degraded in the field. Many parameters affect electromagnetic interactions, and exploring all combinations of parameters is intractable.

Project Goals

LLNL has sophisticated, massively parallel finite element and boundary element codes for solving Maxwell's equations, but many simulations are required to understand how electromagnetic effects vary with circuit layout, frequency, location of the circuit within an enclosure, etc. Our goal is to develop a new method for reducing the complexity, i.e., the computational cost, of this type of parameter-dependent electromagnetic simulation.

Relevance to LLNL Mission

There are numerous national security needs for understanding and predicting electromagnetic effects on circuits. This phenomena is of interest to NNSA NA-42 for detecting and interfering with electronic devices. The DoD has a long-standing interest in high-power microwave systems that use megawatts or gigawatts of radio-frequency (RF) power to disable a hostile system by melting key electrical connections. Clearly, if the more subtle effects that this project aims to study were better understood and could be more

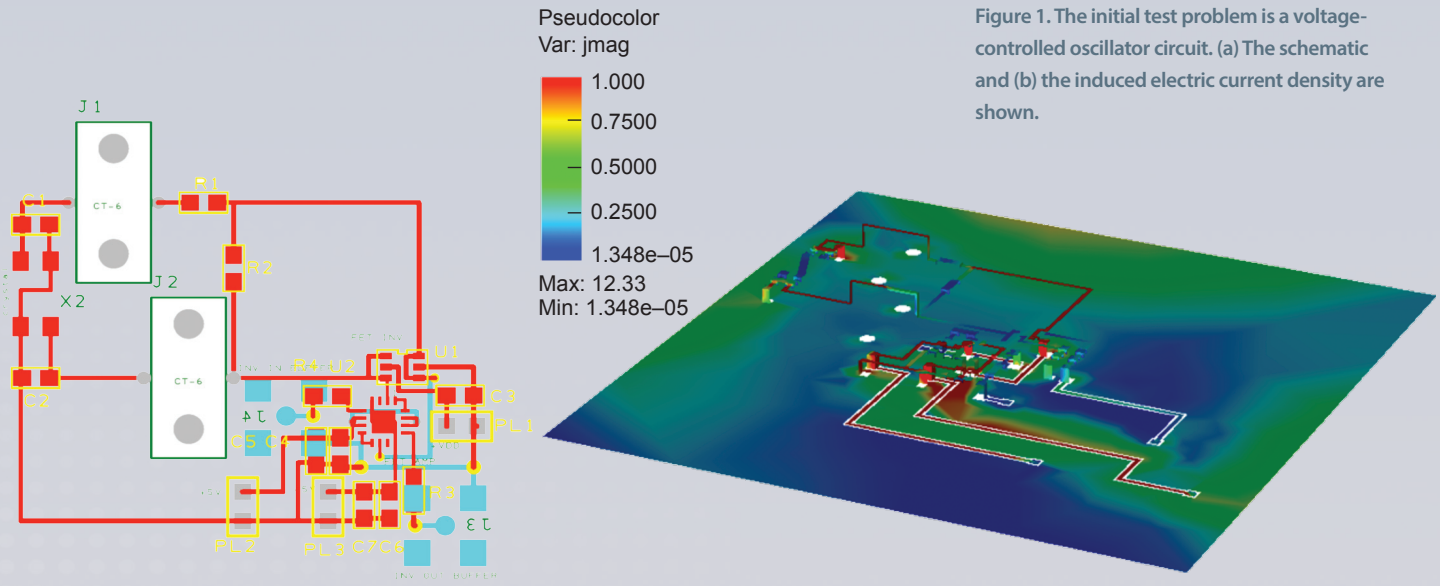

Figure 1. The initial test problem is a voltage-controlled oscillator circuit. (a) The schematic and (b) the induced electric current density are shown.

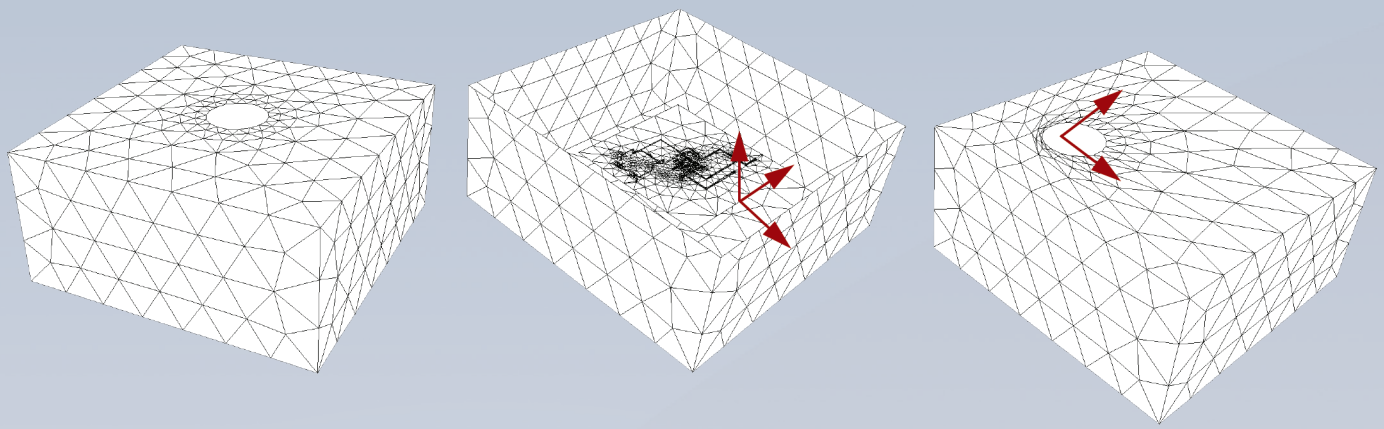

Figure 2. The location of the circuit and the aperture are two variables. (left) The voltage-controlled oscillator circuit is placed in a box with an aperture. (middle) The box is cut away, revealing the circuit and also indicating how the circuit can be moved on any of three axes. (right) A second possible location for the aperture is shown.

reliably achieved, it would be possible to disable a hostile system at a much greater range. In fact, it has been demonstrated that a standard radar can temporary disable an outboard engine-powered motorboat. While several DoD labs are experimenting with high-power microwaves, there is currently no effort to develop computational tools for simulating electromagnetic effects. There is thus an opportunity for LLNL to take the lead on this topic, and if we are successful, our simulations would affect billions of dollars of system development.

FY2012 Accomplishments

We propose to develop automatic model order reduction (MOR) algorithms to reduce the computational cost of performing numerous parameter-dependent simulations. Our starting point is proper orthogonal decomposition combined with radial-basis function interpolation. This reduces an NxN system of equations to an MxM system of equations, with M<<N. The reduced system is so small that it can be evaluated over and over again, for any combination of parameters.

As a test problem, we start with a voltage-controlled oscillator circuit that is known to be shut down when exposed to 500-MHz RF energy (Figure 1). The circuit is placed in a box with an aperture (Figure 2). The location of the circuit within in the box and the location of the aperture are parameters. The goal of this test problem is to compute the electric current density on the oscillator circuit for every combination of parameters.

Let the full complexity finite-element or boundary-element problem be given by the NxN system of equations,

$$\mathbf{A(p)x} = \mathbf{b(p)}$$

where $\mathbf{p} = \{p_1, p_2, ..., p_k\}$ is a vector of parameters, $\mathbf{A(p)}$ is the discrete impedance matrix, $\mathbf{b(p)}$ is the right-hand side vector containing the source terms, and $\mathbf{x}$ is the vector of unknowns. The proper orthogonal decomposition is a change of variables that results in a small MxM system of equations,

$$\mathbf{V^T A(p) V \hat{x}} = \mathbf{V^T b(p)}$$

where $\mathbf{V}$ is a collection of column vectors that spans the important subspace. In our case, $\mathbf{V}$ is formed by solving the full complexity solution for selected parameter values; these are called “snapshots.”

The second step is to accelerate the matrix triple product. This is accomplished via radial basis function interpolation. The idea is to form the expansion

$$\mathbf{V}^{\mathrm{T}}\mathbf{A}(\mathbf{p})\mathbf{V} \approx \sum_{i=1}^{L} \alpha_i(p)\left[\mathbf{V}^{\mathrm{T}}\mathbf{A}\mathbf{V}\right]_i$$

where $\left[\mathbf{V}^{\mathrm{T}}\mathbf{A}\mathbf{V}\right]_i$ is an MxM matrix evaluated at sample point $\mathbf{p}_i$, and $\alpha_i(\mathbf{p})$ is the coefficient of the radial basis function expansion. Solving for the coefficients $\alpha_i(\mathbf{p})$ requires solving an LxL system of equations, but this is done just once, i.e., an off-line step. The LxL system of equations can be ill-conditioned, and understanding and mitigating this issue is a key research issue to be addressed.

One approach for remedying the ill conditioning is to restrict the interpolation size L. This can be done by subdividing the parameter space into subregions and constructing several smaller radial basis function interpolations. This process is illustrated with a 3-parameter example in Figure 3. The parameter space is hierarchically subdivided, and each subregion has its own radial basis function expansion. In this example, parameter space was subdivided into 43 subregions, each with a maximum of 35 sample points for the radial basis function interpolation (i.e., M = 35). Since the dimension of the full-complexity problem is N = 4122, and the solve complexity is $O(N^3)$, this represents a 1000x reduction in the complexity (number of operations) of the problem.

The reduced complexity model does have an error associated with it, which is shown in Figure 3. The error was computed by comparing to the exact solution evaluated at random test points in the parameter space. Ninety percent of the time the error was less than 4%.

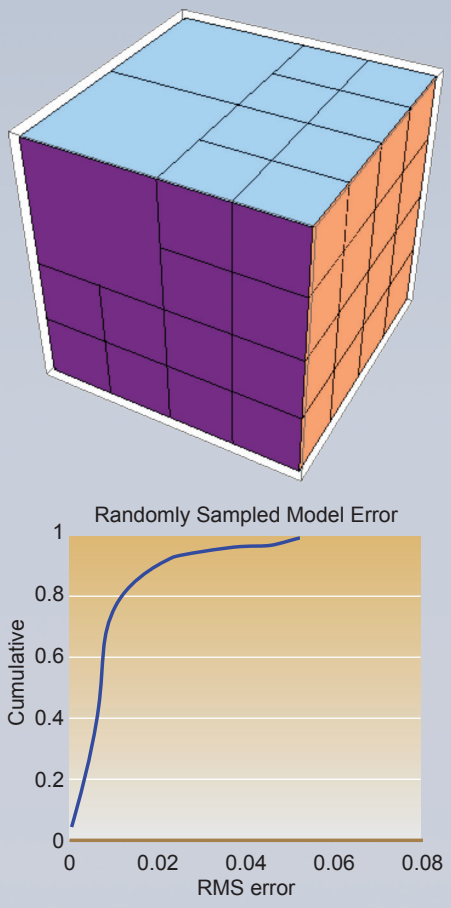

Figure 3. (top) The 3D parameter space has been partitioned into subregions. Each subregion has its own radial basis function expansion. (bottom) This figure shows the cumulative distribution error of the reduced-order model.

FY2013 Proposed Work

For FY2013, we have three goals: 1) continue to investigate the sources of ill-conditioning of the radial basis function interpolation matrix, 2) investigate other interpolation methods such as the recently invented empirical interpolation method, and 3) continue to test the algorithm by applying it to large-scale finite element problems. During FY2013, we expect to be able to achieve a ten-fold reduction in the error of the reduced-order model.

Related References

1. M. Stephanson, J. F. Lee, D. A. White , "Automatic black-box model order reduction using radial basis functions," *IEEE Trans, Ant. Prop. Int. Symposium*, 2011.
2. M. Stephanson, *Adaptive Black Box Model Order Reduction using Radial Basis Functions*, Ph.D. Dissertation, The Ohio State University, 2012.
3. M. Buhman, *Radial Basis Functions*, Cambridge University Press, 2009.

Dan White

Electromagnetics Code Enhancements

Project Overview

It is quite common for engineers to perform high-fidelity simulations (e.g., three-dimensional (3D) finite element codes) over and over again with different initial conditions, boundary conditions, materials properties, or geometry. The goal is sometimes optimization, other times uncertainty quantification, or simply a "what if" conceptual study. In any case, performing numerous related simulations can be computationally expensive. Model Order Reduction (MOR) is a new numerical technique that accelerates this type of calculation. LLNL had a collaboration with The Ohio State University to develop MOR software, and now the goal is to apply and evaluate this methodology.

Project Goals

Previously, MOR was applied to an electromagnetic compatibility problem. Electromagnetic compatibility involves quantifying the undesirable effects of electromagnetic waves on the operation of circuits. The electromagnetic compatibility problem was modeled using the frequency domain boundary element code EIGER, and MOR was used to reduce the required number of EIGER solutions. We investigated applying MOR to finite element solutions of optical waveguides with the goal to determine the geometry that optimizes the dominant electromagnetic eigenmode. This required coupling the MOR software with the EMSolve eigenmode solver.

Relevance to LLNL Mission

With effective MOR technology, LLNL can perform analyses that cannot be performed by commercial codes. This allows Engineering to better support programs. Having a unique

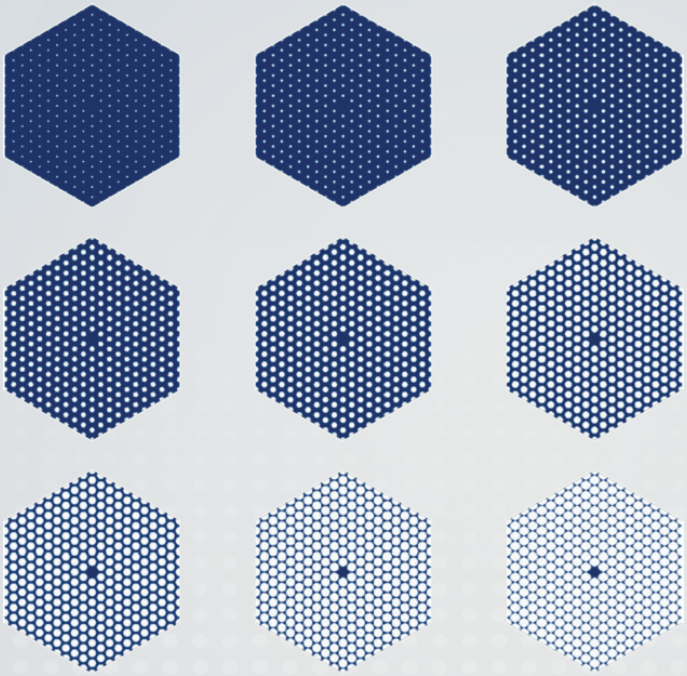

Figure 1. Photonic crystal fiber with varying hole geometry.

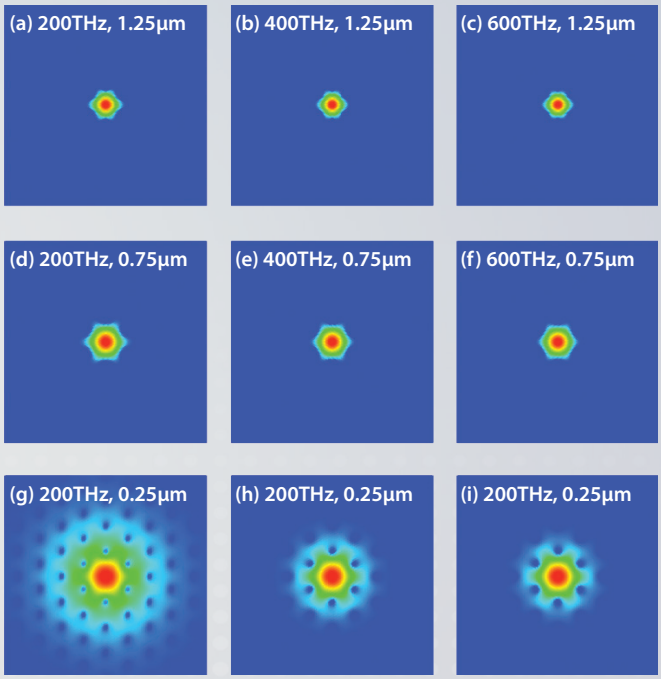

Figure 2. Dominant eigenmodes for various hole sizes and frequencies.

computational MOR capability also allows LLNL to have a competitive edge when competing for DOE and work-for-others projects. Increasing the accuracy and efficiency of our finite element simulations will benefit all customers. The particular application of MOR investigated here—optimization of optical waveguides—is relevant to numerous projects that use high-power lasers.

FY2012 Accomplishments and Results

Simulation of an optical waveguide requires a 2D electromagnetic mode solver. The transverse electric flux density, DT, is given by

$$k^2 \frac{1}{\epsilon} \vec{D}_T = \nabla_T \left(\frac{1}{\epsilon} \nabla_T \cdot \vec{D}_T \right) - \nabla_T \left(\nabla_T \times \frac{1}{\epsilon} \vec{D}_T \right) + \omega^2 \mu \vec{D}_T$$

with the dispersion relation

$$\omega^2 = \frac{1}{\epsilon \mu} \left(k^2 + k_T^2 \right)$$

where ω is the frequency, k is the longitudinal wavenumber, and kT is the transverse wavenumber. Propagating modes have w2 > 0. We are interested in the lowest propagating (or fundamental) mode. The geometry is discretized using a triangular mesh, and the wave equation is solved using the Galerkin finite element method with twisted 1 form basis functions, giving the matrix eigenvalue problem

$$A.x = \lambda B.x \quad \text{where} \quad \begin{cases} A &= \omega^2 M_T(\mu) + S_T\left(\epsilon^{-1}\right) \\ & \quad -M_1(\mu) T_{01} M_0^{-1}(\mu) T_{01}^T M_T\left(\epsilon^{-1}\right) \\ B &= M_T(\epsilon^{-1}) \\ \lambda &= k^2 \end{cases}$$

The matrices M and S above are “mass” and “stiffness” matrices, respectively. The geometry of the optical waveguide, a photonic crystal fiber configuration, is shown in Figure 1. The fiber consists of glass with relative permittivity of 2.25, and holes with permittivity of 1.0. The size of the holes is a parameter to be varied. The frequency is also a parameter; we vary the frequency from 200 to 600 THz (roughly 500 to 1500 nm, from near infrared through green light). A brute-force calculation using 50 different hole sizes and 50 different frequencies would require over 13 days of continuous computing on a 12-processor computer. Instead, we use MOR to accelerate this process. Using MOR, this parameter study can be completed within minutes. MOR is an approximation, but for this application we have confirmed that the approximation is valid to better than 1%. Example computed eigenmodes are shown in Figure 2. These results are relevant to many projects that require high power density optical fibers.

Related References

1. F. Poli, F., A. Cucinotta, S. Selleri, *Photonic Crystal Fibers: Properties and Applications*, Springer, 2007.
2. Stephanson, M., J.F. Lee, D.A. White, “Automatic black-box model order reduction using radial basis functions,” *IEEE Trans, Ant. Prop. Int. Symposium*, July 2011.
3. White, D., M. Stephanson, K. Lange, J.F. Lee, “Application of Model Order Reduction to Multi-Parameter Electromagnetic Compatibility Modeling,” *IEEE Microwave Theory and Techniques*, in press.
4. Stephanson, M., *Adaptive Black Box Model Order Reduction using Radial Basis Functions*, Ph.D. Dissertation, The Ohio State University, 2012.

Domingo Colon

Secure Virtual Network Enclaves (SVNE)

Project Overview

The omnipresent threat posed by a diverse array of malicious cyber hackers has significantly increased the difficulty of carrying out secure computing operations on traditional computer network environments. The Secure Virtual Network Enclave (SVNE) project seeks to research and develop the capability to dynamically create mission-purposed network enclave environments that are intrinsically capable of enforcing a pre-defined, mission-specified security profile. The SVNE platform uses a novel combination of defensive security metric evaluation heuristics and next-generation, proactive defensive capabilities (moving target defense algorithms) that allows enclave environments to be reconfigured and re-tasked "on the fly" to mitigate any identified threat.

Project Goals

Our goal is to develop a methodology and supporting framework for dynamically provisioning virtual network enclave environments that are capable of ensuring an adherence to a mission-specified security profile.

The capability will allow mission planners to create computing environments on-demand with security profiles appropriate to the defined mission of the enclave. Mission planners will be able to formally express a custom definition for each mission, including a methodology for explicitly enumerating the appropriate network and host-based security controls.

Providing a formal means for defining each instance of a "mission" allows the system to automate the task of auto-generating (1) required virtualization resources and (2) metric collection components tailored to the specific instance of the requested enclave. Upon completion of the project, the SVNE framework will accept a definition for a mission, provision the necessary computing infrastructure to support the mission,

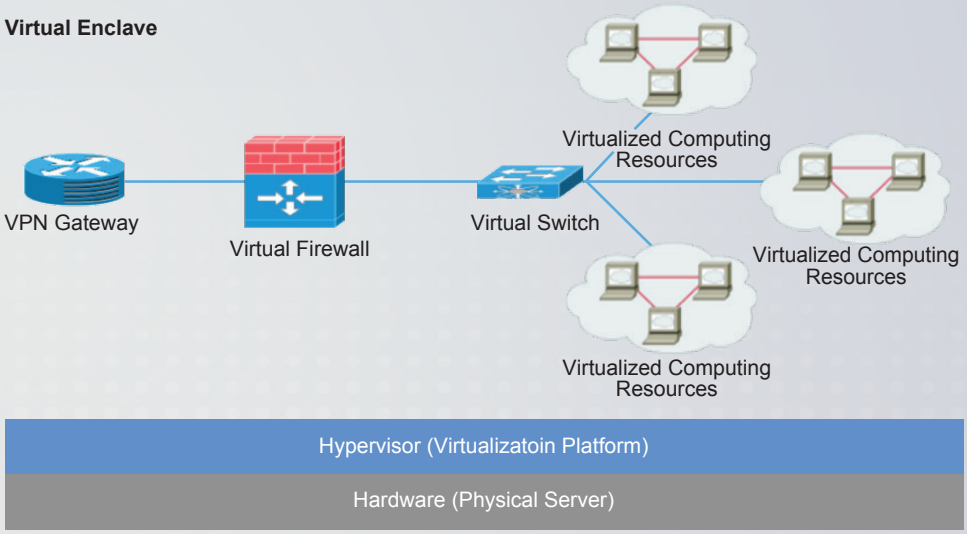

Figure 1. All components of the virtual network are hosted within the hypervisor.

extract a definition of security for the specified operations, generate a custom collection of environment measurement controls to enforce the monitoring of the working security model for the mission, and provide the capability to process the results of the measurement collection components and adjust the operation of the enclave environment.

The central contributions of this effort are three-fold:

- The development of a collection of unique metrics that determine the magnitude and impact of deviations from the mission-specified security policies.
- A novel, ontologically driven methodology for correlating SVNE metrics.
- A configuration synthesis algorithm that is capable of processing the results of the various SVNE metrics and rebuilding the supporting enclave environment such that the mission-specified security properties are upheld.

Relevance to LLNL Mission

If successful, we will have the first true capability to establish secure virtual enclaves in a manner that is useful for operational purposes, as well as for test and evaluation purposes. This capability is a top DoD priority. It also can be used by DOE and any other sponsor that needs to securely operationalize virtual network and cloud technologies to meet core mission requirements.

FY2012 Accomplishments and Results

Major accomplishments for this year fell into five areas. We developed techniques for defining a virtual enclave environment from the perspective of a network focused on security. We explored and identified characteristics that are unique to purely virtualized environments and that form the basis for novel, out-of-band security measurement approaches. We began the process of defining and implementing custom measurement techniques that are capable of enforcing mission-specific security policies at a high level of granularity. We also formalized a system design that will allow measurement components to be provisioned on a custom, per-enclave basis in support of mission-defined security controls. Finally, we developed the capability to instantiate a fully operational virtual representation of a computer network from a formal representation (model) of a desired computing environment.

Figure 2. Enc;lave components are auto-generated from a formal definition of a mission.

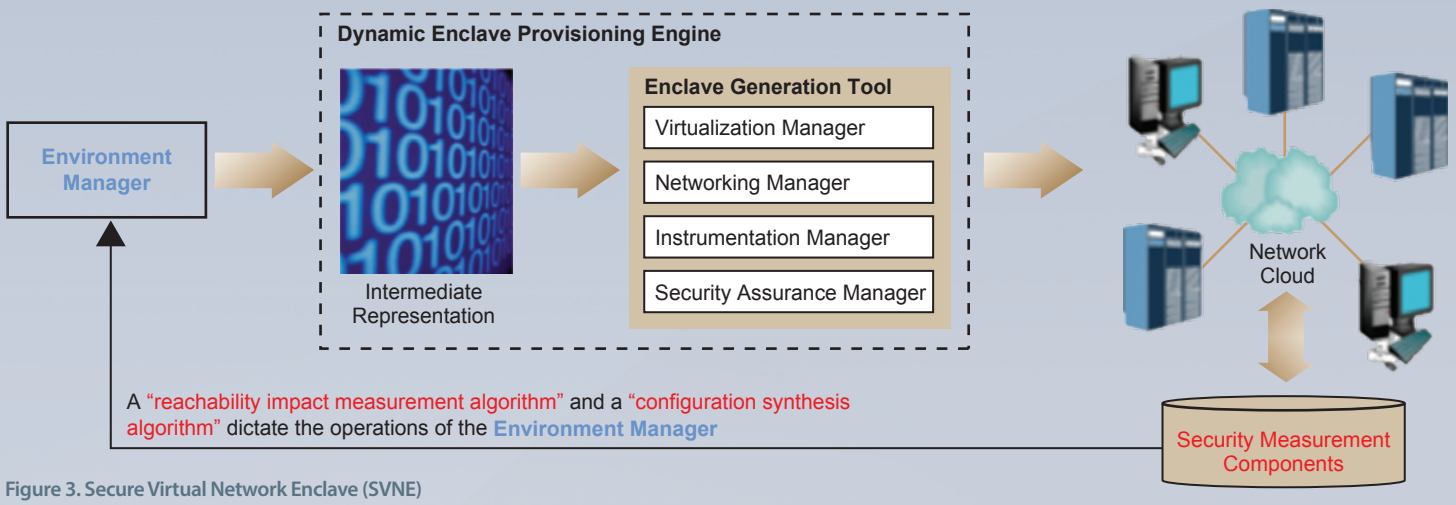

Figure 3. Secure Virtual Network Enclave (SVNE) architecture.

FY2013 Proposed Work

In FY2013 we will explore the notion of a distributed, secure virtual enclave environment. Specifically, we will:

- Develop algorithms and technical approaches for measuring the impact of security policy violations.
- Develop graph analytic-based metrics that calculate the reachability properties of an enclave environment.
- Define the core "configuration synthesis algorithm" and supporting subsystem, which will allow the system to dynamically update the enclave infrastructure to thwart identified security threats.

Related References

1. Manadhata, P., and J.M. Wing, "Measuring a system's attack surface," No. Cmu-Cs-04-102, Carnegie-Mellon Univ Pittsburgh PA School Of Computer Science, 2004.
2. Chu, Matthew et al. "Visualizing attack graphs, reachability, and trust relationships with NAVIGATOR," *Proceedings of the Seventh International Symposium on Visualization for Cyber Security*, ACM, 2010.
3. Rui Zhuang, Su Zhang, Scott A. DeLoach, Xinming Ou, and Anoop Singhal, "Simulation-based Approaches to Studying Effectiveness of Moving-Target Network Defense," *National Symposium on Moving Target Research*, June 11, 2012, Annapolis, MD.
4. Payne, Bryan D., "Simplifying virtual machine introspection using LibVMI," No. SAND2012-7818, Sandia National Laboratories, 2012.
5. Al-Shaer, Ehab, Latifur Khan, and Mohammad Salim Ahmed, "A comprehensive objective network security metric framework for proactive security configuration," *Proceedings of the 4th annual workshop on Cyber security and information intelligence research: developing strategies to meet the cyber security and information intelligence challenges ahead*, ACM, 2008.
6. Ou, Xinming, Wayne F. Boyer, and Miles A. McQueen, "A scalable approach to attack graph generation," *Proceedings of the 13th ACM conference on Computer and communications security*, ACM, 2006.

Adaptive Sampling Theory for Very-High-Throughput Data Streams

Ana Paula
De Oliveira Sales

Project Overview

Predictive modeling based on probabilistic models underlies all manner of modern data analysis tasks, including clustering, classification, regression, and anomaly detection. This project is motivated by the observation that the state of the art in predictive model design is far ahead of the state of the art in predictive model deployment. This is largely due to persistent advances in data collection capabilities: modern data sources are highly dimensional, high frequency, and essentially continuously observed. The reality of such data is that only sequentially computed, online statistical learning methods will be capable of providing real-time situational awareness and decision support for many modern applications.

Project Goals

The goal of this research is to create innovative computational learning algorithms that will enable the use of sophisticated predictive modeling techniques on modern streaming data sources. Over the course of this project, we will pursue an aggressive research agenda involving algorithmic innovation that aims to substantially boost the data ingestion rates of online learning systems. This effort includes developing alternative predictive models for accomplishing standard learning tasks at a fraction of the computational cost and designing new self-adapting learning algorithms capable of automatically adjusting their computational characteristics in order to accommodate target data throughput at minimal expense to prediction accuracy.

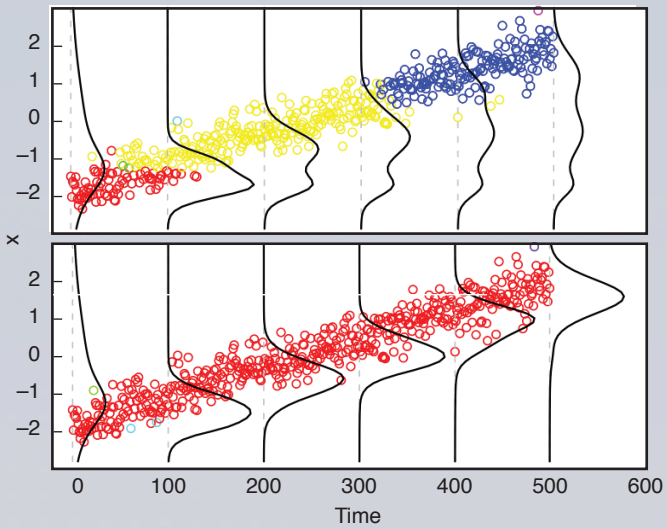

Figure 1. Data density estimated (shown as vertical black lines) by a PF assuming stationary data (top panel) and a dynamic PF assuming concept-drift data (bottom panel).

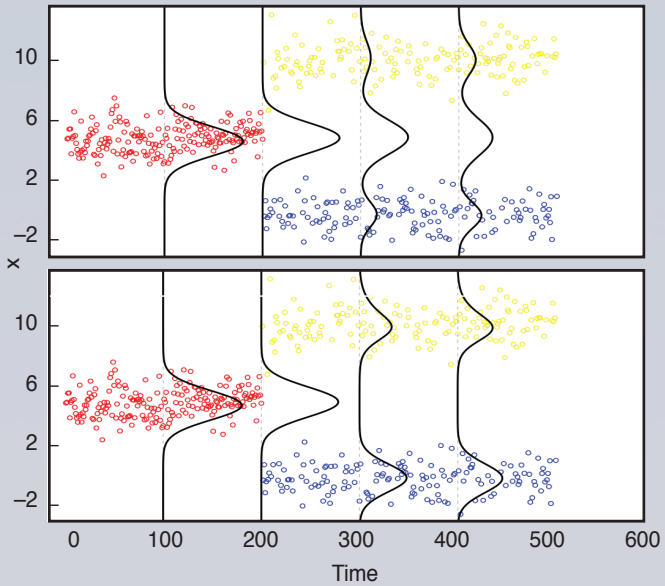

Figure 2. Data density estimated (shown as vertical black lines) by a PF without split-merge capability (top panel) and a dynamic PF with split-merge capability (bottom panel).

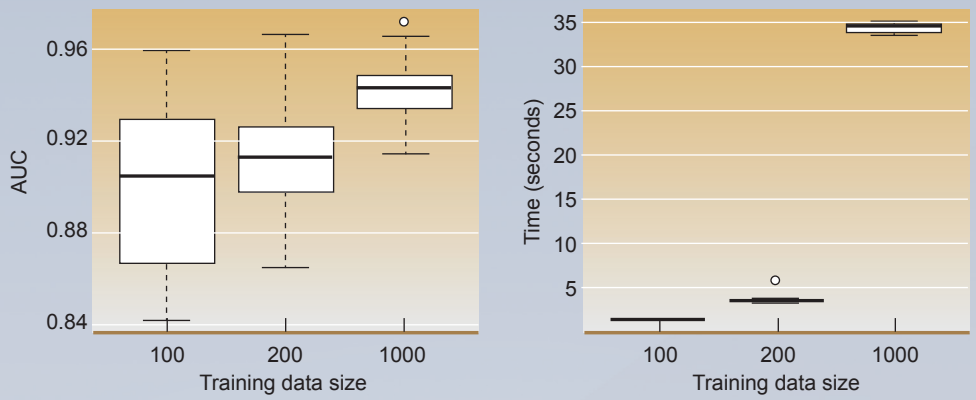

Figure 3. Comparison of the computational and predictive performances of PFs trained on varying amounts of data. The results of this benchmark study suggest that use of AS to down-select data used to update a PF can lead to great gains in computational performance, at little to no cost in predictive performance.

Relevance to LLNL Mission

The "big data" problem alluded to above is pervasive across the LLNL mission space, but it is particularly applicable to the Cyber, Space, and Intelligence (CSI) thrust area and the emerging Energy Systematics (CES21) programs. Both areas are characterized by large, distributed systems producing large, continuously available, distributed data sources. This work seeks to advance our ability to effectively anticipate, detect, and respond to relevant changes in those data feeds.

FY2012 Accomplishments

Our primary goal was to develop new dynamic particle filters (PFs) that automatically adjust to fit time-evolving data. This feature is important for keeping PFs as a broadly applicable analytical tool because for many, if not most, types of streaming data, features of the data are expected to change over time. Dynamic particle filters capable of analyzing time-evolving, concept-drift data were achieved by combining two approaches: 1) implementation of a "forgetting" factor that differentially weights recent data (Figure 1) and 2) development of "split-merge" of mixture components into the model (Figure 2). Additionally, we focused on evaluating and benchmarking the performance of PFs trained with decreasing amounts of data (Figure 3). This benchmark study will serve as a performance baseline for the adaptive-sampling PFs that we have proposed to develop in FY2013.

FY2013 Proposed Work

Our goal is to significantly increase our tools' data analysis rates to address the high data throughput rates in streaming applications. We will pursue this goal with architectural and algorithmic approaches. From the architectural standpoint, we will implement PF in Storm, a massively parallel, high-throughput framework facilitating the processing of enormous amounts of data on the fly. Storm has the benefit of being free and open-source, which is important in ensuring that our system continues to be a readily and easily deployable tool. From the algorithmic standpoint, we will explore adaptive sampling (AS) criteria to increase scalability of a PF. AS will be used to selectively choose observations that arrive in the stream.

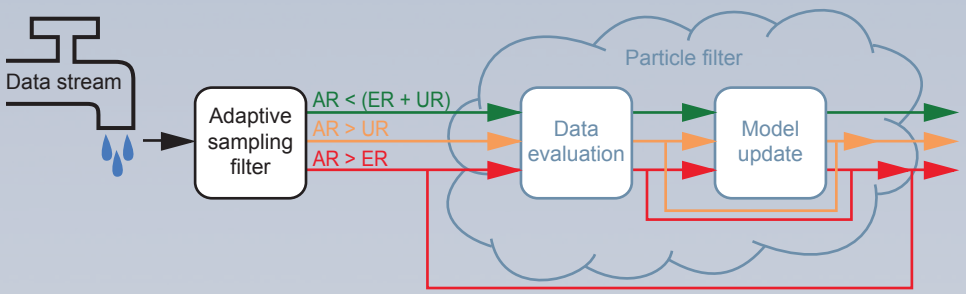

Figure 4. Integration of an adaptive sampler (AS) filter into a PF will allow PF to automatically adapt to the data stream arrival rate (AR). For each observation that arrives, PF performs two primary tasks: data evaluation (i.e., assignment of label) and model update, where the latter is the most computationally intensive step. When data arrival rate is slower than the rate with which PF can fully process an observation, all observations are sent through PF. When AR is faster than the model update rate (UR), AS shuttles most of the data only through the evaluation step, and only the most informative data points are also used in the model update step. Likewise, when AR overwhelms even the data evaluation rate (ER), AS intelligently selects observations to not send through PF.

In situations in which data arrival rates overwhelm a PF's data processing rates, updates to the model will be restricted primarily to those that maximize information gain (Figure 4). Storm and AS are complementary approaches for speedups that will help us achieve orders-of-magnitude increases in data throughput.

Related References

1. Sales, A.P. et al., *Semisupervised Classification of Texts Using Particle Learning for Probabilistic Automata*, Lawrence Livermore National Laboratory, LLNL-JRNL-513511.
2. Dahl, D., "Sequentially-Allocated Merge-Split Sampler for Conjugate and Nonconjugate Dirichlet Process Mixture Models," *Journal of Computational and Graphical Statistics*, 2005.
3. Carvalho, C. et al., "Particle Learning for General Mixtures," *Bayesian Analysis*, 2010.

Tom Edmunds

Large-Scale Optimization Methods for Electric Power Systems

Project Overview

Planning and operation of an electric power grid with large contributions from intermittent renewable resources requires characterization of uncertainty and solution of large-scale, nonlinear, stochastic optimization problems. This project seeks to develop new solution methods and to demonstrate them on high-performance computing (HPC) platforms.

Project Goals

The goal is to develop new tools that support three grid planning and operations areas. The first is weather forecasting methods that represent the uncertainty in renewable generation, as an ensemble of possible weather trajectories is needed. These weather trajectories must be converted to possible electric power generation trajectories using models of wind turbines, and solar photovoltaic and solar thermal plants.

Second, the possible renewable generation trajectories and characteristics of other grid resources must be passed to a stochastic optimization algorithm to minimize the expected costs of operating the grid with respect to the trajectories. The optimization problem includes both integer decision variables (e.g., when to turn plants on and off) and continuous variables (e.g., the power level of each plant). A linearized version of the nonlinear power flow problem is used for this formulation. Typical problems in industry are of a large scale, involving up to a million decision variables.

Third, methods for solving smaller-scale instances of the nonlinear optimal power flow problem are needed. Semidefinite programming methods have recently been applied to this problem domain with mixed success.

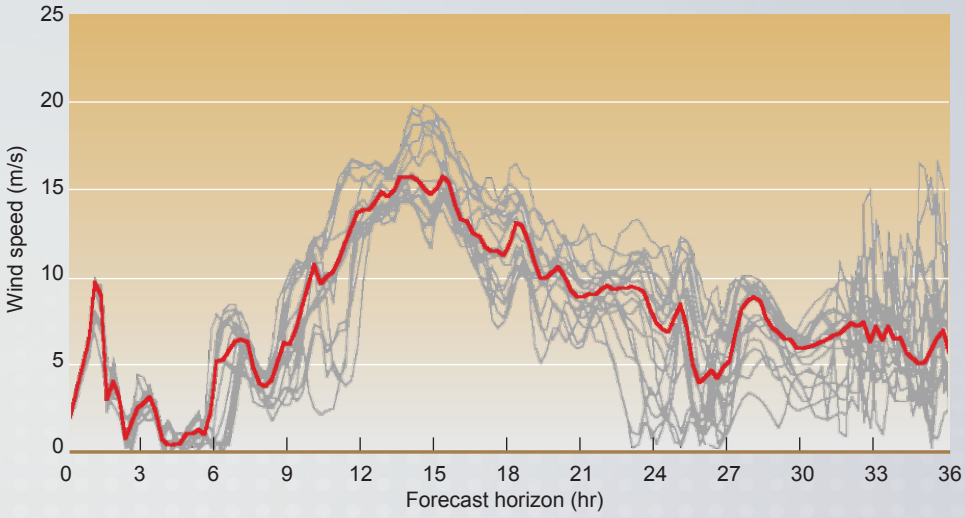

Figure 1. Multiphysics ensemble forecast time series of 100-m wind speed at San Gorgonio wind park on August 1, 2005.

Relevance to LLNL Mission

The project is well aligned with the institutional science and technology plan. The algorithms and codes being developed address programmatic needs for analysis of energy systems. The research is undertaken within the Earth and Environmental Sciences Pillar supporting the Climate and Energy Security Focus Area.

FY2012 Accomplishments and Results

Major accomplishments for this year include modification of the Weather Research and Forecasting (WRF) code to represent weather uncertainty due to alternative physics parameterizations. The code selects 30 different combinations of physics submodels in order to generate 30 weather trajectories for the western United States. These weather trajectories were transformed to renewable generation using models of wind turbines and solar plants, then passed to the two-stage stochastic optimization code, Plexos. LLNL has a research agreement with the developers of Plexos and is the first to use these stochastic optimization functions and deploy the code on HPC systems.

In a second collaborative effort with the University of California at Berkeley, a technique known as Lagrangian relaxation was used to break up the large-scale problem into related subproblems and solve them in parallel. Finally, a semidefinite programming algorithm was implemented, experiments were conducted to solve the nonlinear optimal power flow problem, and numerical stability issues were identified.

Figure 2. Simplified model of the western electrical grid.

FY2013 Proposed Work

We plan to implement Plexos in parallel. An analysis year will be conducted in parallel as 52 separate weeks. Nine days will be used to model each week in order to reduce the impact of end effects. We will also solve larger-scale, two-stage stochastic programming problems using the Lagrangian relaxation technique on machines with more cores. This work will help secure approval of the proposed utility-funded $150 million research effort known as California Energy Systems for the 21st Century (CES-21).

Related References

1. Epperly, T. et al., "High Performance Computing for Electric Grid Planning and Operations," *Proceedings of the IEEE Power and Energy Society Conference*, August 2012.
2. Santiago, C., "A Note on the Paper Zero Duality Gap in Optimal Power Flow Problem," *IEEE Transactions on Power Systems*, in review.
3. Lamont, A., "Assessing the Economic Value and Optimal Structure of Large-scale Electricity Storage," *IEEE Transactions on Power Systems*, in review.
4. Papavasiliou, A. and S. Oren, "Applying High Performance Computing to Multi-Area Stochastic Unit Commitment for Renewable Penetration," accepted by *Mathematical Programming*.
5. Papavasiliou, A. and S. Oren, "Multi-area Stochastic Unit Commitment for High Wind Penetration in a Transmission Constrained Network," accepted by *Journal of Operations Research*.

Noah Goldstein

Livermore Energy Systems Assessment

Project Overview

The electrical grid is changing rapidly, as new technology, economic conditions, and legislation shape infrastructure and the deployment of new analytical tools. Understanding the capabilities of these new technologies is critical for LLNL to advance its national security mission and to operate as a high-performing applied research facility. LLNL is in fact using its own sites as a "sandbox" for testing and exploring innovations that promote sustainable facility practices and improve energy-related capabilities.

The two sites offer very different environments. Site 200, the main site in Livermore, comprises hundreds of buildings housing highly specific and elaborate research facilities, including the National Ignition Facility and the Terascale Simulation Facility, the heart of Livermore supercomputing. Maintaining electrical continuity and high quality is paramount for day-to-day operations and ongoing national security applications. East of the main site lies the rural Site 300, a landscape of steep terrain, developed for testing high explosives. DOE has recently encouraged using areas like Site 300 for renewable energy generation. LLNL is extending that mandate to study the deployment of advanced electrical grid equipment and sensors at both sites to further renewable and grid forecasting and diagnostics.

Project Goals

This project examined ways that the two sites, and Site 300 in particular, could be used to advance energy-related research and funding opportunities. The two major components of the project are electric grid diagnostics and solar power evaluation.

Figure 1. Google Earth rendering of GridLab D model showing site power use at Site 200.

Relevance to LLNL Mission

Improving LLNL's sustainability and energy capabilities promotes our energy security mission area. Any new capabilities implemented as part of this work will benefit Global Security's E Program research as well as the institutional energy efficiency and sustainability goals of the O&B Principal Associate Directorate.

FY2012 Accomplishments and Results

Part of the electric grid diagnostics effort included developing a rendering of the site electrical grid using the GridLab-D simulation package. This effort led to a model of about 4300 components on Site 200, including high-voltage equipment and building energy meters. The model was linked with the site's OSISoft PI data archive, enabling a dynamic view of energy use of site facilities.

We also deployed and analyzed readings from Phasor Measurement Units (PMU), a key indicator of phase and quality on electrical grids, as shown in Figure 2. Upcoming projects with electric utility providers will rely on integrating hundreds of PMUs; this effort enabled LLNL to get a head start on electrical power analysis and multiple PMU

integration, using the site and data source. The PMU experiment also prepared LLNL for streaming data, a challenging component of smart grid analysis.

In order to assess the research relevance of solar power deployment at Site 300, we conducted an analysis of the industry need for solar forecasting. The potential stakeholders included the solar manufacturing industry, electrical power generators, independent system operators, and electric utilities. The study sought to balance current forecasting capabilities, different forecasting horizons, and the computational gaps that exist. This work resulted in a funded California Energy Commission project, in which we will collaborate with forecasting solar power to load balancing at the building scale.

FY2013 Proposed Work

In FY2013, efforts will focus on expanding expertise for fine-grained electrical monitoring and modeling, and working with the electrical utilities to better understand their technical and computational challenges.

Related References

1. Wang, D., et. al, "A test bed for self-regulating distribution systems: Modeling integrated renewable energy and demand response in the GridLAB-D/MATLAB environment," *Proceedings of the Innovative Smart Grid Technologies (ISGT), 2012 IEEE PES*, 2012.

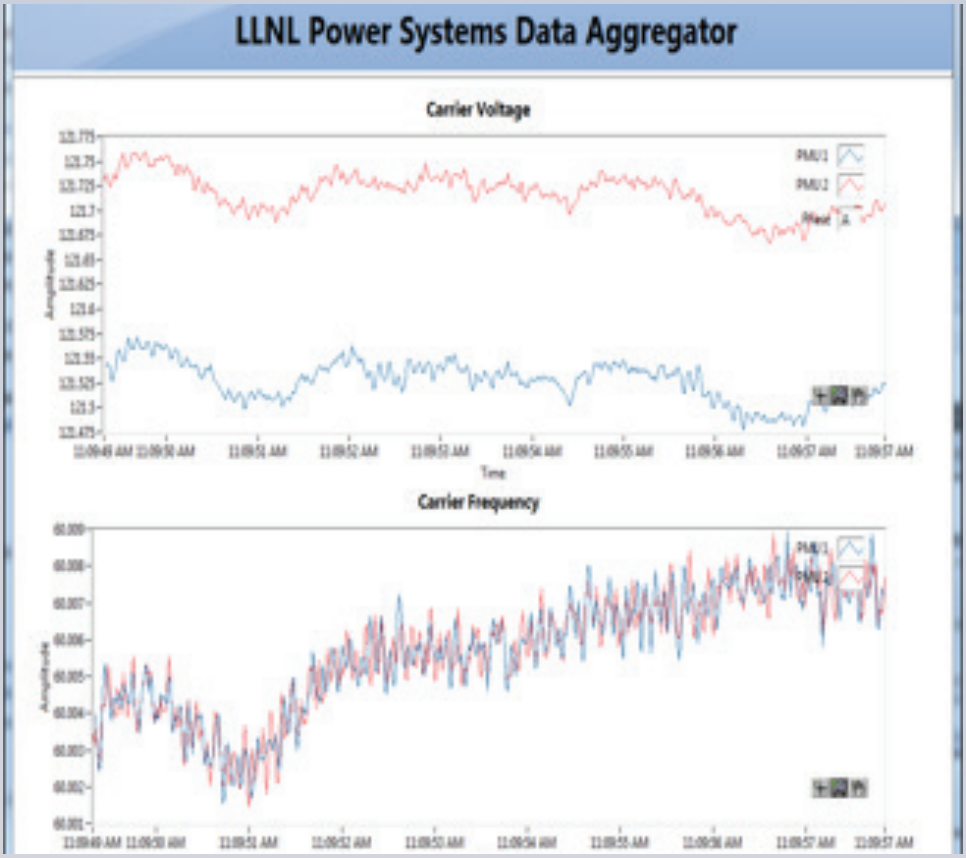

Figure 2. Screenshot from LLNL PMU data aggregator.

Noah Goldstein

The Livermore Energy Systems Informatics Capability

Project Overview

In virtually every corner of business, science, and government, there is talk about "Big Data." The opportunity and fear of the coming tsunami—or fire hose (choose your metaphor)—of structured and unstructured data has elevated raw bits from the inner workings of analysis and decision-making to the centerpiece of better system design and problem solving. The big-data situation is no different in the case of the network of power generation, transmission, and distribution systems that is our energy grid. A truly innovative energy system is set to evolve and become "smart" to incorporate today's technology, regulations, and dynamic economic markets. For such an evolution, new approaches to data storage, analysis, integration, and visualization are essential.

The Livermore Energy Systems Informatics Capability (LESIC) is designed to enable an evolution of the traditional grid to a "smart" grid. Multiple stakeholders at LLNL recognized that we need common approaches to data, big and otherwise, in the energy system to assure the Lab will be ready for the coming onslaught of data and projects needing this capability. One such project is the California Energy Systems for the 21st Century, or CES-21, a ratepayer-funded initiative, in which the three largest California Investor Owned Utilities, or IOUs, will fund LLNL and its partners $150 million over five years to tackle large problems in electrical and gas infrastructure planning and operations. LESIC began as a way to assist current projects and initiatives in energy data science and management and has evolved to address the collective needs of landmark big-data projects for LLNL. LESIC could only be accomplished as a collaborative effort, and has been led by Engineering and co-funded by Global Security and Computation.

Project Goals

The goal of LESIC is to establish a common capability for energy systems informatics that will assist current projects and develop new projects that leverage current capabilities. LESIC has three major components:

- Consolidation and coordination
- Analysis and simulation
- Distribution and visualization

For each of these areas, LESIC seeks to develop a new mission-focused project, assist a current project to achieve its goals, or develop a new method of data storage, analysis, or visualization.

Relevance to LLNL Mission

This project is directly aligned with the strategic goals in LLNL's Energy and Climate focus area. The capabilities implemented in this work will benefit multiple programs, including Global Security's E Program (DOE, EERE), and applied research in Global Security, Computation, and Engineering (LDRD and State of California smart grid and renewable energy programs).

FY2012 Accomplishments and Results

During this past year, in the area of consolidation and coordination, we developed a comprehensive data lifecycle management (DLM) system to create and collect, store, model, retrieve, analyze, and visualize project-based data sources. Working with multiple organizations within LLNL, we were able to stand up a robust yet flexible architecture and repository for energy systems data (Figure 1).

For analysis and simulation, we expanded the domain of building energy simulation and examined interstate energy exports and imports. To support LLNL's effort in accelerating the path to exascale computing, we explored the design of a new computing facility to be placed in the Livermore Valley Open Campus (LVOC). Called the LVOC Computing Center (LVOC-CC), this new computer facility would place significant demands on site energy use; by simulating design and material options, more efficient options could be explored. Over 51,000 simulations of a year's energy performance of the LVOC-CC were run, using 100 CPU hours. From this analysis, the benefits of very efficient building chillers and selecting appropriate temperature setpoints became clear. In addition, other constraints, such as building insulation materials, showed less impact than previously assumed (Figure 2).

Work on distribution and visualization entailed creating an extensible portal service for relevant stakeholders. This prototype was created to better understand current approaches to data service at LLNL, accounting for the sensitivity and needs of upcoming projects, like CES-21.

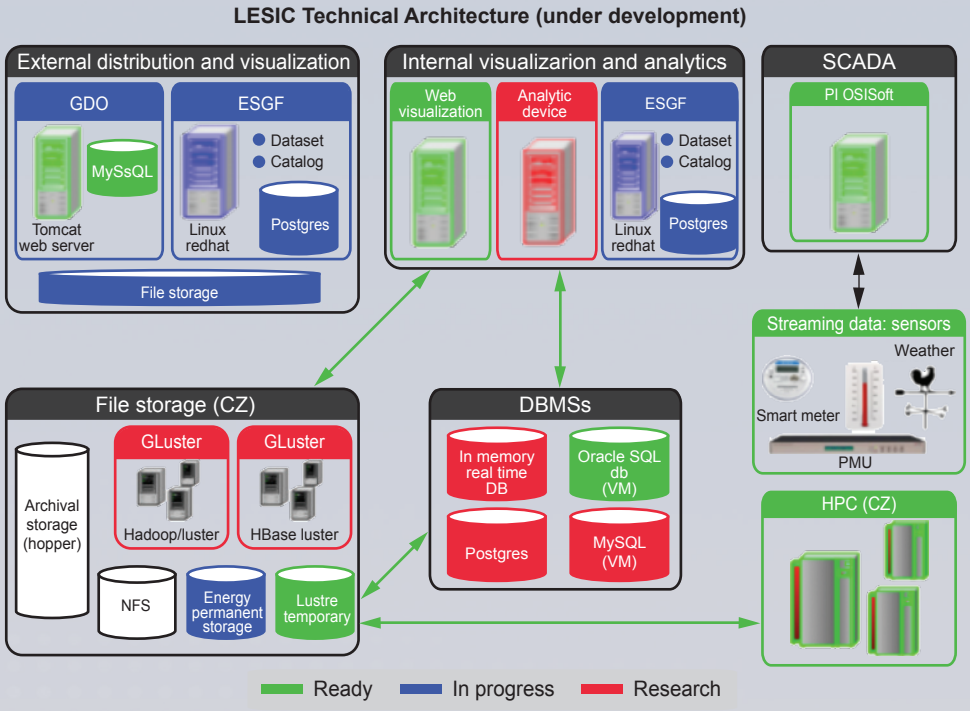

Figure 1. A representation of the LESIC technical architecture.

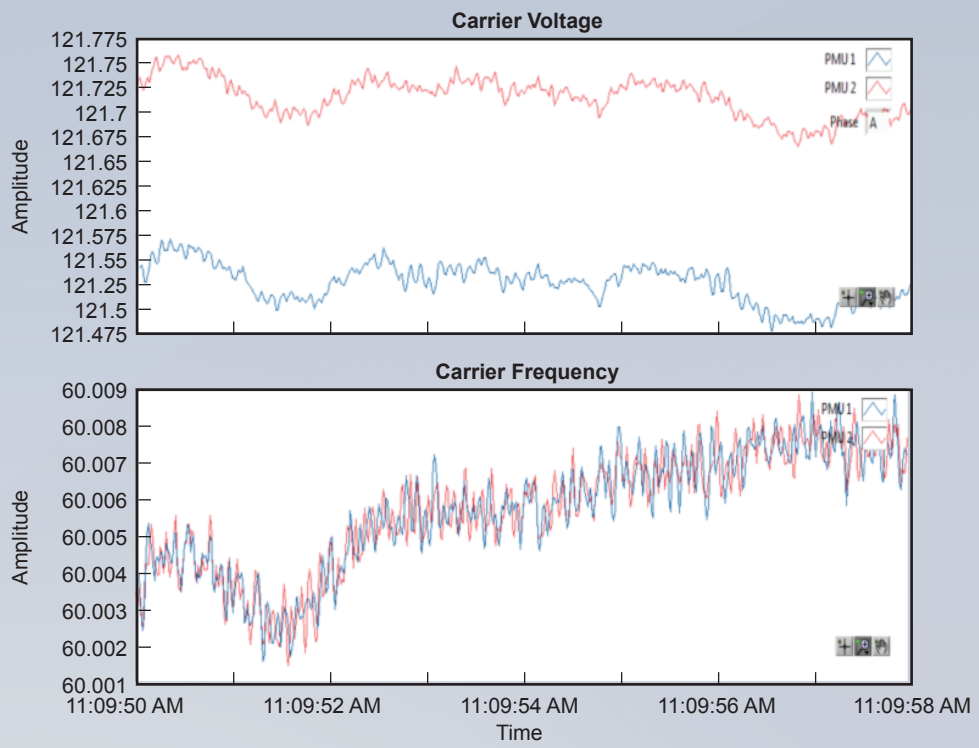

Figure 2. Graphs showing the results of over 51,000 runs of the LVOC-CC using the Energy Plus software.

FY2013 Proposed Work

In the coming year, we will extend LESIC in multiple ways, including:

- Creating data models and metadata standards for energy systems data for LLNL projects in grid management, renewable energy forecasting, demand response, energy flows, and building energy use.
- Advancing dynamic models of the electrical grid for the Western region and the LLNL site.
- Continuing discussions with energy systems stakeholders, namely the California utilities, on their data, modeling, and security challenges.
- Creating collaborations with key educational partners in energy systems informatics.

Related References

1. Attia, S., E. Gratia, A. De Herde, J. L.M. Hensen, "Simulation-based decision support tool for early stages of zero-energy building design," *Energy and Buildings*, 49, 2–15, June 2012. ISSN 0378-7788, 10.1016/j.enbuild.2012.01.028.
2. Sutter, M., V. Hartmann, M. Götter, J. van Wezel, A. Trunov, T. Jejkal, R. Stotzka, "File systems and access technologies for the large scale data facility," *INGRID 2010: Instrumenting the Grid*, 2010.
3. Watson, R. T., M-C. Boudreau, M-C., A.J. Chen, "Information Systems and Environmentally Sustainable Development: Energy Informatics and New Directions for the IS Community," *MIS Quarterly* **34**:1, 23–38, 2010.

Medical Diagnostics

Reg Beer

Project Overview

Ongoing mission needs in biosurveillance and force protection include rapidly detecting and diagnosing infectious disease in the field or forward-deployed area. This operational space demands diagnostics that are rugged, inexpensive, and robust while still maintaining expected performance standards. The goal for this project has been to develop inexpensive and portable approaches to molecular diagnostics, as well as label-free optical detection methods to reduce the power, size, and footprint of molecular diagnostic instruments.

Project Goals

Project goals have been to:

- Develop a disposable polymer-based sample preparation consumable concept for a small, portable polymerase chain reaction (PCR) instrument.
- Develop a multiplexed, febrile illness reactive antigen protein microarray utilizing serodiagnostic assays on microarray printers, in collaboration with the Felgner Laboratory at University of California at Irvine (UC Irvine).
- Develop a fast PCR prototype with optical detection.
- Investigate label-free detection methods to reduce the expense and complexity of field-based fluorescence detection.

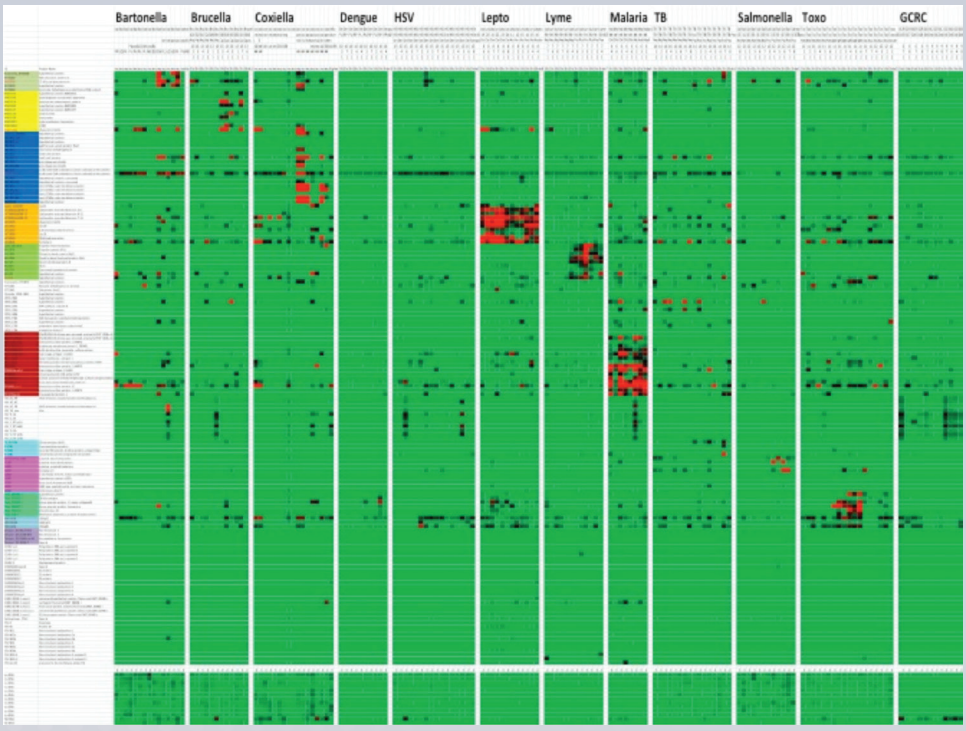

Figure 1. Heat map of fever stick hybridization showing "diagonal" of non-cross-reactive proteins.

Relevance to LLNL Mission

Increasing the flexibility and performance characteristics, and lowering the cost of specific and accurate molecular diagnostics, is key to the nation's strategy of force protection and global outreach. Our technical approach has allowed for newly developed technologies to mature to the point where they can be proposed for programmatic needs in the biodefense arena. Additionally, we selected our platform to provide maximum flexibility by advancing both nucleic acid and protein-based diagnostic strategies.

FY2012 Accomplishments and Results

In FY2012, the team:

1) Developed an 18-organism febrile illness "Fever Stick" protein microarray with UC Irvine:
   - Panel: malaria parasites, viral hemorrhagic fevers, HIV, TB, dengue, and other bacteria and disease-causing parasites
   - Successfully tested on human clinical samples at UC Irvine
2) Designed an optical "real-time" detection system for fast PCR.
3) Tested a label-free optical detection system for DNA microarrays using the Femtosense USB reader technology.

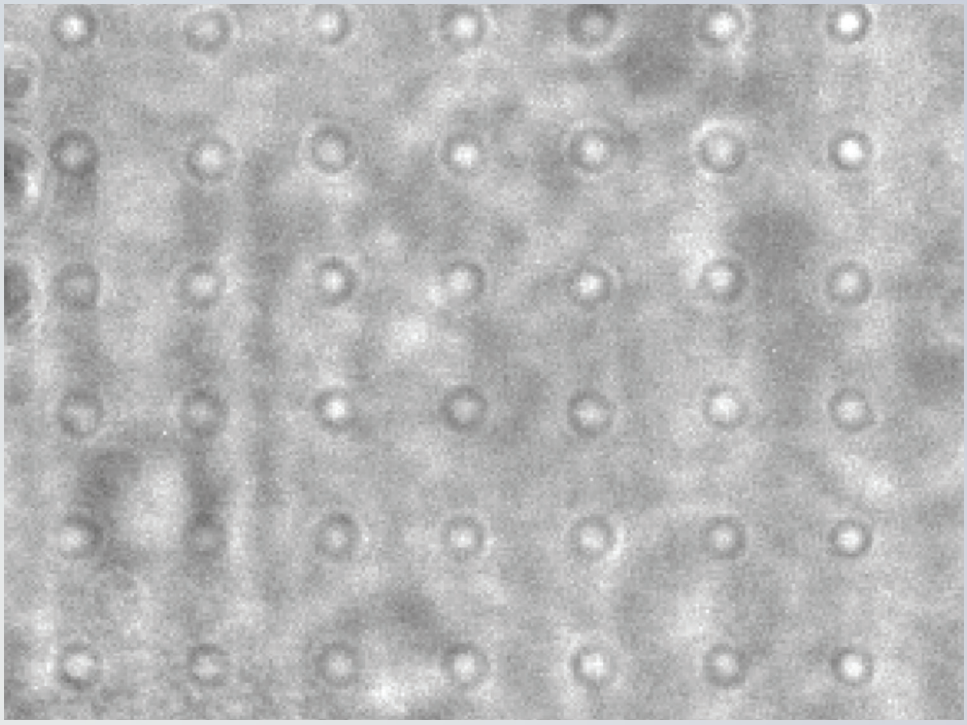

Figure 2. First measurements with optical interferometry detection of microarray spots show features in a 4-µm region. This label-free detection method is being investigated in collaboration with Femtosense Inc.

Subwavelength Plasmon Laser Arrays

Tiziana Bond

Project Overview

Plasmon lasers represent the next generation of coherent optical amplifiers for significantly enhancing nanoscale interactions of light and matter. Although only a few plasmonic nanolasers have been reported—limited to a single standalone nanocavity—our aim is to produce multiple devices, arranged in arrays, that leverage our recent developments in tunable plasmonic nanocavity platforms.

Project Goals

The goal of this project is to develop plasmonic-based ultracompact lasers that can directly generate coherent optical fields at the nanometer scale, far beyond the diffraction limit. These deep-sub-wavelength-sized lasers are built upon plasmonic nanocavities that support shorter wavelength surface plasmons—electromagnetic (EM) surface charge density waves at the interface between metal and dielectric media—extending only a few nanometers. By bouncing this highly confined light within nanogap resonators, the conditions for enhanced spontaneous emission are achievable, even with modest optical feedback. This development could enable performances comparable and even superior to those obtained in standard lasers.

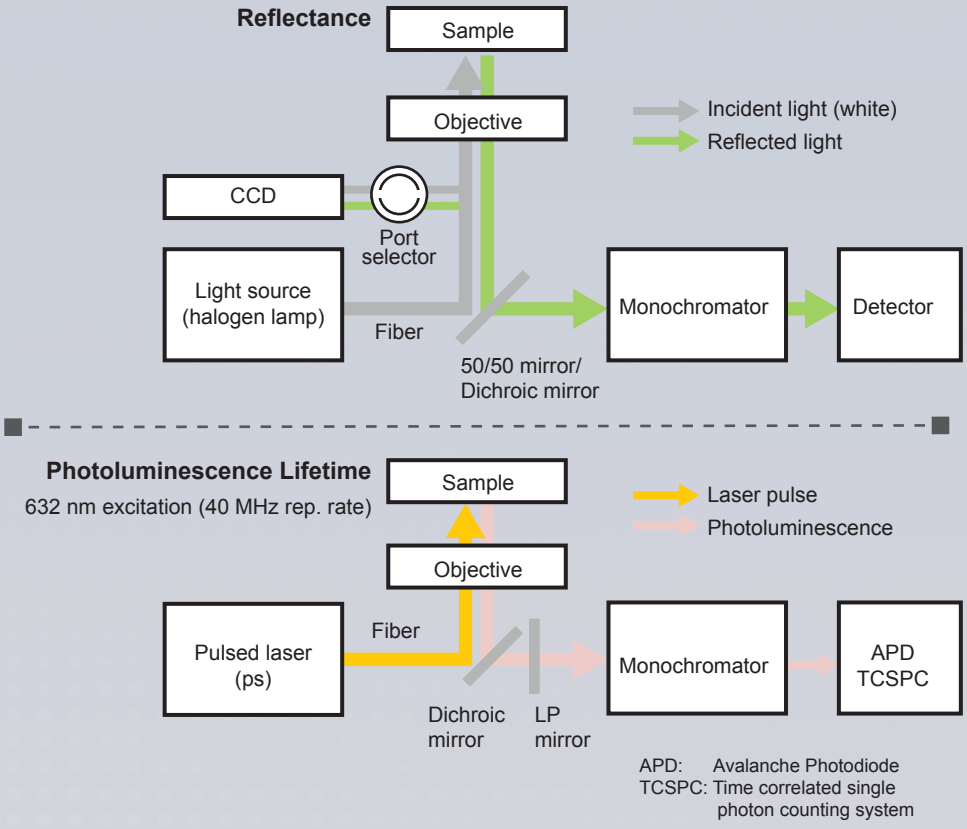

Figure 1. (top) Schematic and (bottom) setup for simultaneous reflectance and PL lifetime measurements.

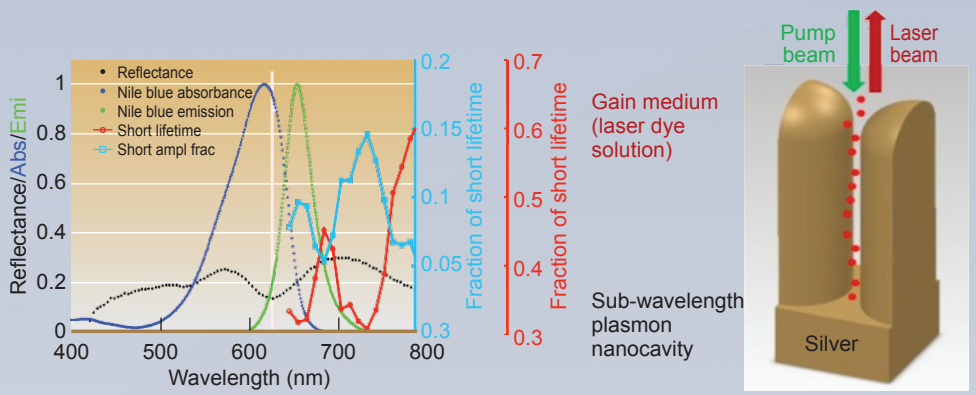

Figure 2. (a) The short lifetime (light blue) within nanocavities is reduced to ~ 0.06 ns (~20x reduction with respect to pristine dye lifetime, ~1.1 ns). The fraction of short lifetime (number of photons that had a short lifetime) increased at the same time. Nanopillar reflectance spectra (black dotted line) shows resonance (dip) at 650 nm, aligned to the pumping source (pink line) and closely located to the maximum peak of the Nile Blue absorbance. (b) Schematic of the unit cell of the periodic nanopillar substrate and principle of operation.

We can attain laser arrays on a large scale by leveraging our tunable plasmonic nanocavity platform that is currently produced on 4" wafers. The core of the project is to provide a proof-of-concept for optically pumped nanolaser arrays by embedding the substrate with gain material. Given our ability to define multiple resonances in our metallic nanopillar structures, we plan to align them with both the absorption and emission spectra of the gain media, to enhance the dipole cross-section and decay rates. One item on the critical path is to create emission conditions by appropriate loss-gain balance, i.e., for radiative decay channels to overcome nonradiative (lossy) ones.

Relevance to LLNL Mission

This frontier research to extend plasmonic-based, ultracompact lasers to arrays will be a game-changer in many fields highly relevant to the Laboratory's national security mission: compact spectroscopy, high-power sources, embedded sensing, data storage, highly dense optical interconnects, and advanced manufacturing at the nanoscale.

FY2012 Accomplishments and Results

We have focused on the design and fabrication of metallic nanopillar arrays with plasmonic resonances that match either the absorption or the emission of the gain media. (Figure 1) The need is to separately investigate each effect. Furthermore, we developed the necessary measurement setups, including a pulsed, white-light source with 50-fs pulse widths (MHZ repetition rates) over a 400–800 nm range, to enable the excitation of various resonances. We also developed a reflectometry/time-resolved PL system that enables the simultaneous characterization of hotspot EM and dye-emission properties.

Initial results provided confidence in the platform's potential. (Figure 2) Time-resolved PL of Nile-Blue pumped at 63 nm revealed the presence of a decay channel with a higher decay rate than is encountered in bulk conditions. The fast decay rate is wavelength-dependent, which indicates the influence of plasmonic resonances. The highest increases in fast decay rates of 20× (on par with literature) and fast decay amplitudes—which is up to 45%—were recorded at the same wavelengths, indicating that the faster decay is mainly associated with radiative rather than nonradiative channels.

FY2013 Proposed Work

Our efforts in FY2013 include investigating:

- The correlation of reduced lifetime and increased PL with plasmonic resonances as a function of wavelength excitation and input power.
- Near-field optical amplitude and power measurements to uncover the plasmon density of states in the cavities.
- Rate equations to help evaluate decay channels.
- Possible conditions for enhancing modal spontaneous emission.

Related References

1. Noginov, M.A. et al., "Demonstration of a spaser-based nanolaser," *Nature* 460, 1110, 2009; Oulton, R.F. et al., "Plasmon lasers at deep subwavelength scale," *Nature* 461, 629, 2010; Ma R-M. et al., "Room-temperature sub-diffraction-limited plasmon laser by total internal reflection," *Nature Materials* 10, 110–113, 2011.
2. Bora, M., B. Fasenfest, E. Behymer, A. Chang, H.T. Nguyen, J.A. Britten, C. Larson, T.C. Bond, "Vertical pillar array plasmon cavities," *Nano Lett.* 10, 2832, 2010; Gartia, M.R., Z. Xu, E. Behymer, H. Nguyen, J.A. Britten, C. Larson, R. Miles, M. Bora, A. Chang, T.C. Bond, G.L. Liu, "Rigorous surface enhanced Raman spectral characterization of large-area high-uniformity silver-coated tapered silica nanopillar arrays," *Nanotechnology* 21, 395701, 2010.
3. K. Munechika, M. Bora, E.M. Behymer, D. Dehlinger, J. Britten, C.C. Larson, A. S-P Chang, H.T. Nguyen, T. Bond, "Enhanced Photoluminescence in Plasmonic Resonant Nanocavities," *MRS Fall Meeting*, 2013; M. Bora, E.M. Behymer, D. Dehlinger, J. Britten, N. Ileri , A. S-P Chang, H.T. Nguyen, T. Bond, "Black plasmons in metallic resonant cavities," *MRS Fall 2012*; K. Munechika, M. Bora, E.M. Behymer, D. Dehlinger, J. Britten, C.C. Larson, A. S-P Chang, H.T. Nguyen, T. Bond, "Black plasmons in metallic resonant cavities," under review, *Appl. Phys. Lett*.

Jonathan B. Hopkins

Massively Parallel Multi-Axis Micro-Reflector Array for High-Speed Directed Light-Field Projection

Project Overview

The intent of this project is to develop an array of tightly-packed (>99%) micro-mirrors (70 x 70) that may be independently controlled in three axes (tip, tilt, and piston) using closed-loop control at high speeds (40–120 kHz) over large ranges (±10–20 degrees mechanical half-range). The unprecedented capabilities of this array will enable a number of new technologies, such as high-definition multithreaded autostereoscopic displays, bullet-defeat defense shields, and novel, high-speed, multimaterial, additive nano-fabrication processes. The optimal design, which is currently being fabricated at LLNL, is shown in the figure in Figure 1.

Project Goals

The specific goals for this project are to review the capabilities of existing micro-mirror array technologies, determine theoretical performance limits for all general micro-mirror arrays, and design a new array of micro-mirrors with capabilities that surpass those of the current state of the art and approach the theoretical performance limits of general arrays.

Relevance to LLNL Mission

The realization of the proposed mirror array will enable a number of useful applications that are directly applicable to LLNL's mission. The most relevant application is for the LIFE project and beam steering for tracking and igniting the deuterium capsules fired into the fusion chamber. Another application is shooting down close-range, high-speed bullets/projectiles with focused laser beams that are rapidly steered using the mirror array. The mirrors could also be used to simultaneously move, place, and sinter millions of various nanoparticles as three-dimensional printed structures using the principle of optical tweezers. This application directly supports a fabrication initiative in the Center for Micro- and NanoTechnology.

Figure 1. Micro-mirror array and design for a single mirror.

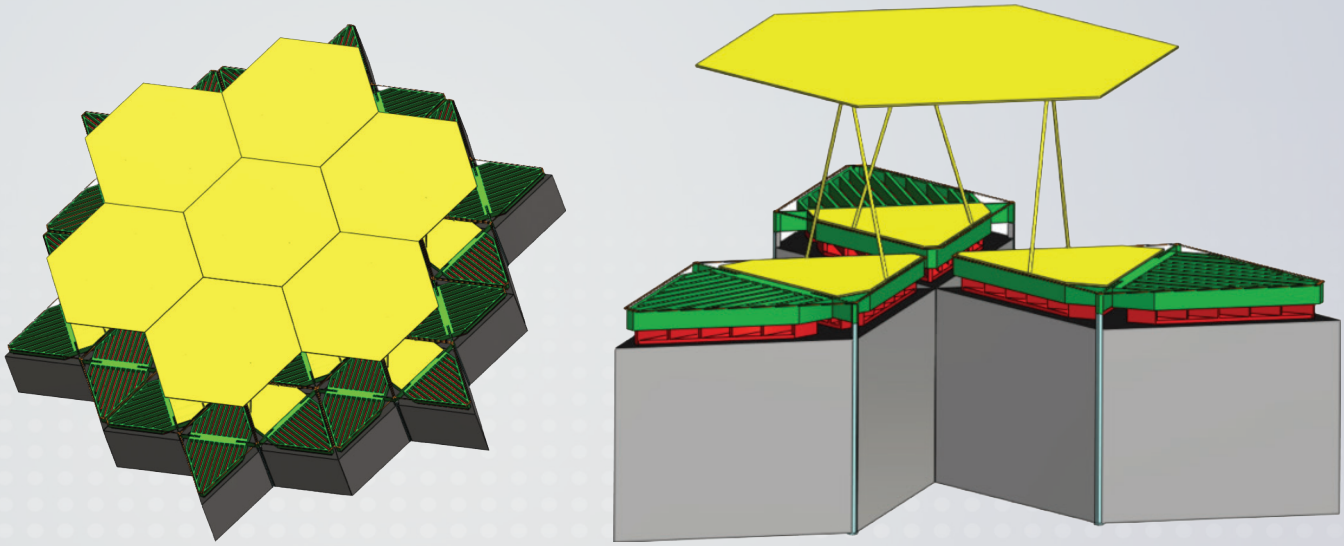

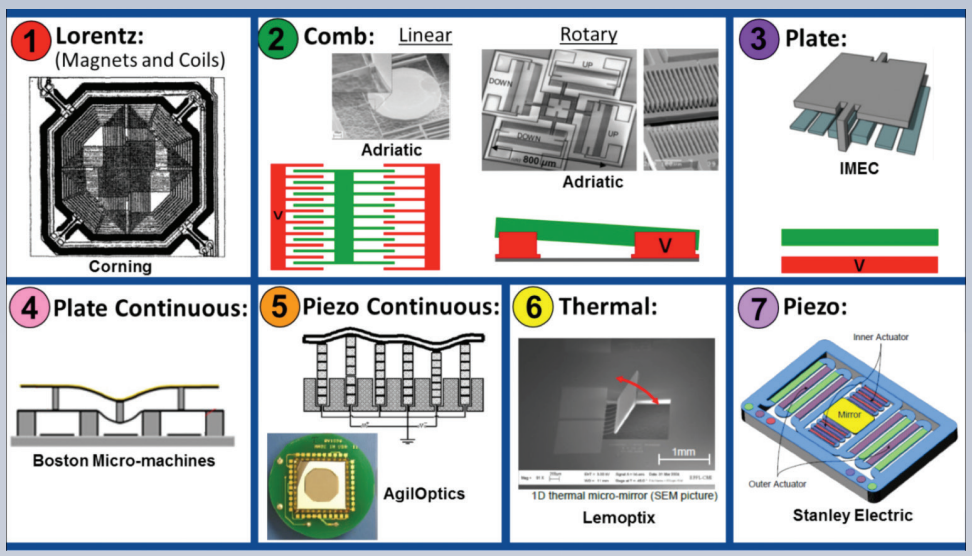

Figure 2: Seven categories of mico-mirror types.

FY2012 Accomplishments and Results

We have reviewed multiple books, 50 articles, and 85 companies that pertain to micro-mirror designs of any type. We classified these existing designs into the seven categories shown in Figure 2. Among these designs, only a few of them may be arrayed, possess at least two degrees of freedom (i.e., tip and tilt), and a fill-factor greater than 75%. The speed and range of these mirror arrays are shown in Figure 3. The mirrors that are circled represent those that can be arrayed only with a small number of mirrors due to fabrication limitations and electrical trace routing issues [1-4]. These mirrors are heavily underconstrained, possess parasitic errors, and utilize control systems to compensate for the issues inherent to their mechanical design. In contrast, the predicted performance of the optimal LLNL design from Figure 1 is indicated by the arrow in Figure 3. Its energy density versus size is also compared with the other competing mirror arrays, as shown in Figure 4. The fundamental energy density performance limit is shown in this figure. Note that the LLNL mirror design approaches this limit and far surpasses the performance capabilities of competing technologies.

FY2013 Proposed Work

In the coming year, we will finish researching and comparing the performance of existing micro-mirror array designs. We will also calculate more useful theoretical limits on the performance of general micro-mirror arrays. Additionally, we will fabricate and test a prototype array of seven mirrors to demonstrate fabrication feasibility and then will fabricate a similar but optimized seven-mirror array to validate its predicted performance.

Related References:

1. Milanovic, V., K. Castelino, "Sub-100 micro-second Settling Time and Low Voltage Operation for Gimbal-less Two-Axis Scanners," *IEEE/LEOS Optical MEMS 2004*, Takamatsu, Japan, August 2004.
2. Milanovic, V., G.A. Matus, D.T. McCormick, "Gimbal-Less Monolithic Silicon Actuators for Tip-Tilt-Piston Micromirror Applications," *IEEE Journal of Selected Topics in Quantum Electronics*, **10**(3): 462–471.
3. Milanovic, V.; Castelino, Kenneth; McCormick, D., "Fully-Functional Tip-Tilt-Piston Micromirror Array," *Optical MEMS and Their Applications Conference*, August 2006.
4. Milanovic, V., Matus, G.A., McCormick, D.T., "Tip-Tilt-Piston Actuators For High Fill-Factor Micromirror Arrays," *Solid-State Sensor, Actuator and Microsystems Workshop*, Hilton Head Island, South Carolina, June 6–10, 2004.

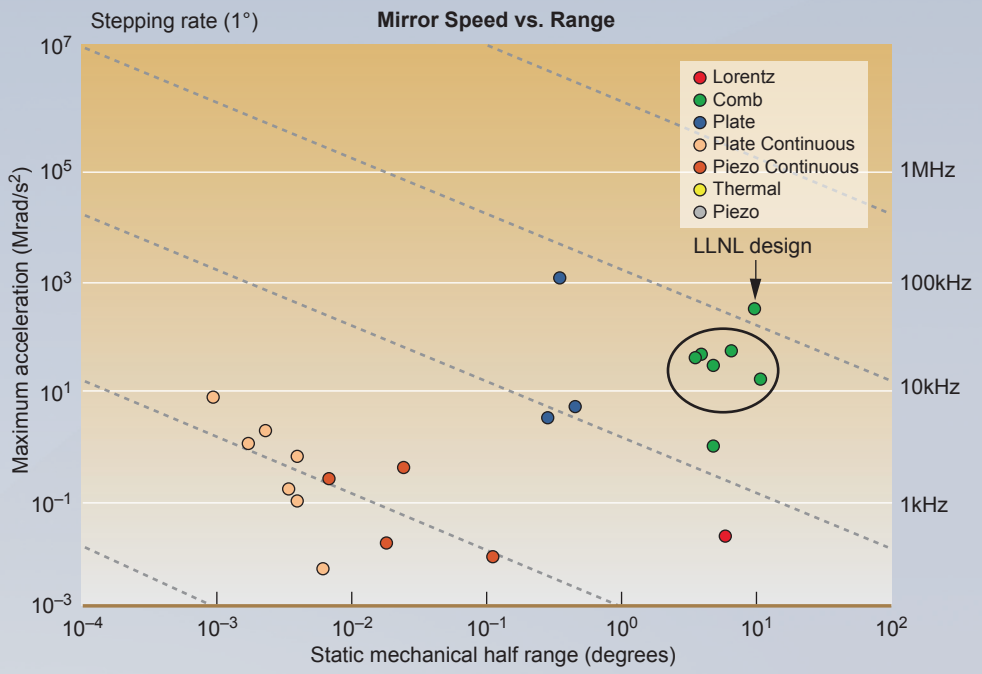

Figure 3: Existing mirrors that can be arrayed, possess at least tip and tilt degrees of freedom, and a fill-factor greater than 75%.

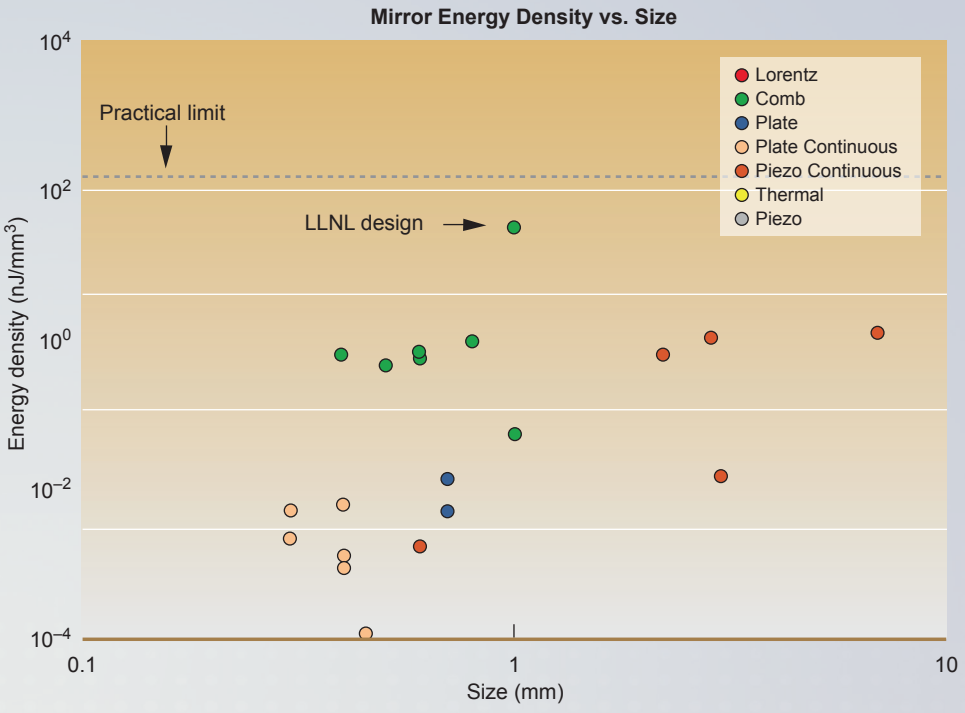

Figure 4: The energy density versus size of existing micro-mirrors.

Embedded Sensors for Monitoring Complex Systems

Jack Kotovsky

Project Overview

As the nation's nuclear stockpile is reduced in size, stockpile surveillance approaches must change to increase safety, security, and cost effectiveness. For this purpose, this effort pursued broad-specie gas sensing to monitor the evolution of chemical species throughout a weapon system. Specifically, surface enhanced raman spectroscopy (SERS) and photo-acoustic spectroscopy (PAS) systems were explored.

Project Goals

This project developed two new, complementary sensing capabilities, both fiber-optic based. SERS and PAS were developed to detect gas species in a complex, unknown mixture. Novel materials, fabrication processes, and designs were explored for the difficult constraints of in-situ state-of-health stockpile monitoring.

Relevance to LLNL Mission

This project helps lay the groundwork for a game-changing, embedded sensor suite. Ultimately, sensors with capabilities such as these will dramatically enhance stockpile surveillance and change the nuclear weapons complex, supporting the Laboratory's national security and stockpile stewardship missions.

FY2012 Accomplishments and Results

For PAS, our final design iterations showed great progress in improving the PAS gas detection limits. Although COMSOL modeling guided the early design effort, final tuning of the hardware required direct experimentation. Carbon dioxide was used as a test gas to quantify the system's limit of detection (LOD). The resulting system was compared to a commercial electronic CO_2 meter in an enclosed chamber. Varied CO_2 concentrations mixed with air were parametrically evaluated to guide the final geometries of the design (Figures 1 and 2).

The final design consisted of an acoustically tuned gas chamber with both input and output fibers. The single-mode input fiber stimulated the gas mixture under study with frequency modulated laser light. The sample was driven at the resonance of the acoustic chamber, which was matched to the resonance of the acoustic detector. Motion of the detector was interrogated with a laser vibrometer system through the output fiber and optics. The overall length of the acoustic chamber is 75 mm with a 2-mm diameter. These dimensions can be scaled for further size reduction depending on the application demands.

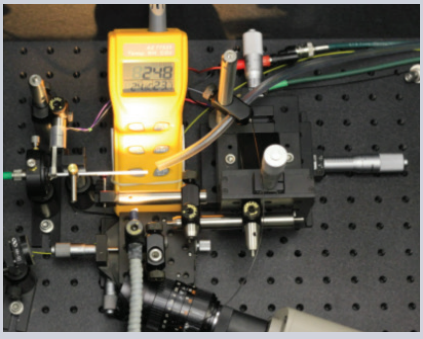

Figure 1. The experimental test setup in the gas enclosure. This benchtop setup was used to characterize different system designs to produce a successful PAS system.

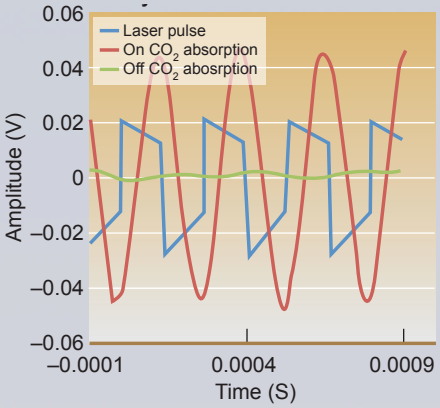

Figure 2. Example data showing the system's voltage output when the driving laser is tuned on and off the CO_2 absorption line. The system can detect 10ppm CO_2 in an air mixture.

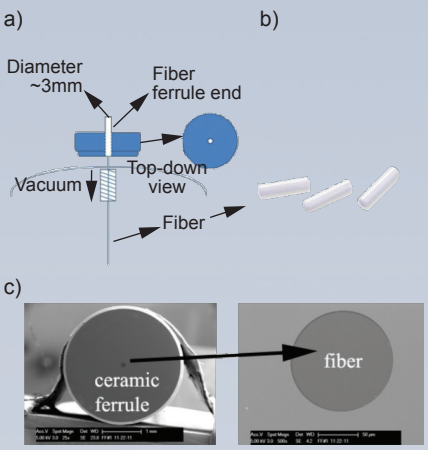

Figure 3. (a) Schematic of the spin coating process for the optical fiber. (b) Photograph of the fiber ferrule. (c) Scanning electron microscope images of the fiber ferrule facet; (d) patterned surface on the fiber core.

For SERS, we achieved multiplexed sensing of vapors at room temperature using our nanopillar templates. Toluene and trichloroethelene were tested in mixed solutions and we demonstrated their simultaneous sensing. Toluene was detected singularly down to 250 ppm, at lower temperatures. Full kinetic studies of adsorption and detection were performed as well. All samples were recoverable after a mild annealing of the substrates. We successfully realized the transfer of these sensitive substrates onto the tip of a standard multimode commercial fiber. Figure 3 shows the basic building platform. We have achieved the integration by mounting a conventional multimode fiber in a ferrule that holds the sample during the fabrication steps. SERS detection was demonstrated in both front-end and back-end interrogation schemes, the latter being most critical for field applications (Figure 4). The fiber-SERS was also proved for both liquid and gas-phase conditions with standard molecules. Our nanostructured fiber has shown excellent detection limits. In fact, the system detected DNT vapors (Figure 4, right), proving a limit of detection down to the ppb concentration level. Furthermore, we showed enhanced Raman detection of three volatile organic vapors by simultaneously flowing them through photonic crystal fibers.

Related References

1. Kotovsky, J., W. Benett, A. Tooker, and J. Alameda, "Micro-Optical-Mechanical System Photoacoustic Spectrometer," Patent Number 8,342,005 B2, January 1, 2013.
2. Yang, X., A.Y. Zhang, D.A. Wheeler, T.C.. Bond, C Gu,, and Y. Li, "Direct Molecule Specific Glucose Detection by Raman Spectroscopy Based on Photonic Crystal Fiber," Anal Bioanal Chem 402, 687–691, 2012.
3. Yang, X. , A.S.P. Chang, B. Chen, C. Gu, and T.C. Bond, "High Sensitivity Multiplexed Gas Sensing by Raman Spectroscopy Using Photonic Crystal Fiber," Sensors and Actuators B, 2012.
4. Yang, X., N. Ileri, C.C. Larson, T.C. Carlson, J.A. Britten, A.S P. Chang, C. Gu, and T.C. Bond, "Nanopillar array on a fiber facet for highly sensitive surface-enhanced Raman scattering," Optics Express 20, 24819–24826, 2012.
5. Yang, X., T.C. Bond, N. Ileri, C.C. Larson, T.C. Carlson, and J.A. Britten, "Nanoscale array structures on optical fiber for surface enhanced Raman scattering," provisional patent.

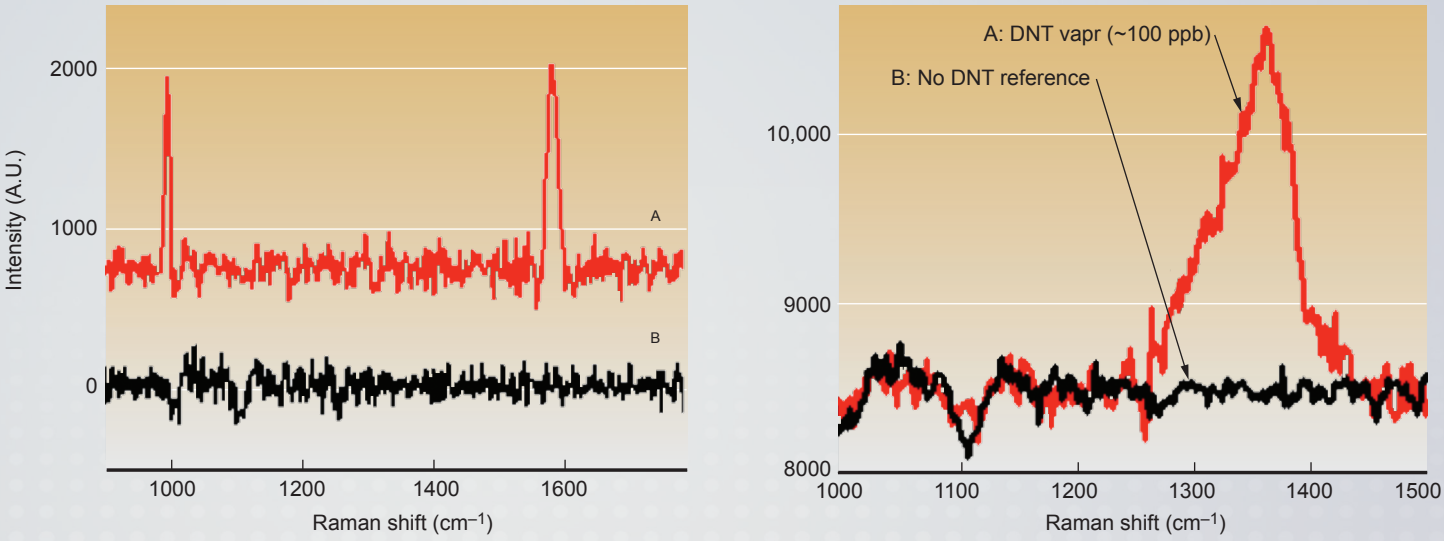

Figure 4. (left) Curve A: the SERS spectrum of the fiber probe for the remote detection of toluene vapor (laser power: 2 mW, integration time: 10 s); Curve B: the spectrum obtained by the unpatterned optical fiber in the toluene vapor with the same system configuration. (right) Curve A spectrum for remote detection of DNT vapor (100-ppb vapor pressure). Curve B: Spectrum obtained using the same configuration with no DNT vapor exposure.

Scalable High-Volume Micro-Manufacturing Techniques for Three-Dimensional Mesoscale Components

Christopher Spadaccini

Project Overview

Our goal is to fundamentally understand and develop, from the ground up, new micro-manufacturing techniques applicable to a variety of materials such as polymers, metals, and ceramics. These techniques would enable production of three-dimensional mesoscale geometries with micrometer-scale precision and scalable to achieve high manufacturing volumes at low cost. Traditional manufacturing processes start with bulk material followed by a forming or metal-removal process. For mesoscale parts, this is time consuming and wasteful in energy and material. In addition, grain size becomes problematic and material handling is difficult. This project will revolutionize the way we manufacture parts for advanced fusion-class laser system targets as well as for myriad other devices.

The design of any new hardware component, regardless of the application, is constrained by the materials available and the geometry that can be fabricated using existing manufacturing processes. We expect to overcome both of these limitations through advanced fabrication processes that are capable of achieving arbitrary three-dimensional mesoscale structures with microscale architectures and sub-micrometer precision. These processes will be revolutionary to manufacturing and have a broad impact because of compatibility with a wide range of materials, rapid translation from computer model to fabricated component, and the ability to scale to large numbers of components. We intend to design and fabricate a “new” material with specified properties such as thermal expansion versus stiffness outside the bounds of those attainable with bulk materials processed via traditional synthesis methods. Success in meeting our proposed objectives will both illustrate capabilities of the process and demonstrate novel materials and structures relevant to LLNL missions and programs.

Project Goals

We have extensive experience developing microfluidic devices made from multilayer stacks of polydimethylsiloxane (PDMS) containing both fluidic and control microchannels. Each additional layer is stacked and bonded to previous layers. In this project, we worked to integrate porous membrane filters into our existing process. We first established a method to bond our membranes between two PDMS layers, without delaminating, while they are exposed to greater-than-expected fluidic pressures. Next, we sought to evaluate the membrane’s efficiency at filtering viruses.

By testing the microfluidic sample preparation modules with forensic samples, we sought to establish this capability within a biosafety level 2 laboratory and evaluate the efficiency of isolating human DNA from complex forensic samples.

Relevance to LLNL Mission

Precision engineering enables Laboratory programs to field experiments and metrology capabilities to advance science and technology in the national interest.
A "bottom-up" three-dimensional manufacturing process combined with multiple materials enables new design concepts that have not been possible and offers cost reduction for advanced fusion-class laser system targets and rapid turnaround for new target designs in support of Livermore missions in stockpile science and reducing or countering threats to national and global security.

FY12 Accomplishments and Results

In FY12 we improved and expanded upon our micro-manufacturing technologies, and our efforts in microcellular materials demonstrated previously unachievable material property combinations. Specifically, we (1) fabricated and characterized micro-lattice architectures with ultrahigh stiffness-to-density ratios and lattices with negative Poisson's ratio, (2) fabricated and characterized binary thermite materials energy release rates spanning two orders of magnitude, (3) produced a three-dimensional mesoscale component with complex geometry, and (4) demonstrated novel structures by combining our micro-manufacturing techniques.

Proposed Work for FY13

In FY13 we will continue to advance our micro-manufacturing techniques by scaling up to produce larger parts, fully incorporating multiple-material capability into several of our systems and designing additional materials with unique microstructures, providing previously unachievable properties. Specifically, we will (1) design a micro-architecture for a negative Poisson's ratio, which will produce a structure that will contract in one direction when compressed in another; (2) fabricate and characterize that structure; (3) establish the capability to fabricate heterogeneous structures with our projection micro-stereolithography system; (4) fabricate and characterize thermite materials with a fully three-dimensional design; and (5) fabricate additional unique components by combining micro-manufacturing technologies.

Publications

1. Duoss, E., et al., 2012. *Additive micro-manufacturing of designer materials*. 3rd Intl. Workshop Young Materials Scientists, Pathumthani, Thailand, Aug. 28–31, 2012. LLNL-PRES-568692-DRAFT
2. Duoss, E., et al., 2011. *Direct-write assembly of functional inks for planar and three-dimensional microstructures*. Composites at Lake Louise VII, Alberta, Canada, Oct. 30–Nov. 4, 2011. LLNL-PRES-508971-DRAFT.
3. Kolesky, D. B., et al., 2011. *Direct-write assembly of micro-energetic materials*. 2011 MRS Fall Mtg. and Exhibit, Boston, MA, Nov. 28–Dec. 2, 2011. LLNL-POST-523435.
4. Kuntz, J. D., et al., 2011. *Colloidal crystal assembly by electrophoretic deposition—Experiments and modeling*. Technologies for Future Micro–Nano Manufacturing, Napa, CA, Aug. 8–10, 2011. LLNL-POST-491953.

5. Olson, T. Y., et al., 2012. *Controlled synthesis of fluorapatite nanorods for directed self assembly by electrophoretic deposition*. 2012 Spring MRS Mtg., San Francisco, CA, Apr. 9–13, 2012. LLNL-POST-543471.
6. Olson, T. Y., et al., 2012. *One-dimensional nanostructures: Growth mechanism, assembly manipulation, and materials applications*. 23rd Conf. Crystal Growth and Epitaxy–West, Fallen Leaf Lake, CA, June 3–6, 2012. LLNL-ABS-552344.
7. Olson , T. Y., et al., 2012. "Shape control synthesis of fluorapatite structures based on supersaturation: Prismatic nanowires, ellipsoids, star, and aggregate formation." *Cryst. Eng. Comm*. **14**, 6384. LLNL-JRNL-557031-DRAFT.
8. Orme, C. A., et al., 2012. *Controlled synthesis of fluorapatite nanorods for directed self-assembly by electrophoretic deposition*. Nanotech Conf. and Expo 2012, Santa Clara, CA, June 18–21, 2012. LLNL-ABS-528495.
9. Pascall, A. J., K. T. Sullivan, and J. D. Kuntz, 2012. *Edge effects in electrophoretic deposition*. 65th Ann. Mtg. APS Division of Fluid Mechanics, San Diego, CA, Nov. 18–20, 2012. LLNL-PRES-601912-DRAFT.
10. Pascall, A. J., K. T. Sullivan, and J. D. Kuntz, 2012. "Morphology of electrophoretically deposited films on electrode strips." *J. Phys. Chem. B*, **117**(6), 1702. LLNL-JRNL-560451.
11. Pascall, A. J., et al., 2011. *Electrophoretic deposition for the fabrication of materials with designer microstructure via dynamic electrodes and electric field sculpting*. 2011 MRS Fall Mtg. and Exhibit, Boston, MA, Nov. 28–Dec. 3, 2011. LLNL-PRES-515011.
12. Pascall, A. J., et al., 2012. *Electrophoretic deposition for the fabrication of materials with novel properties through microstructural control*. Nanotech Conf. and Expo 2012, Santa Clara, CA, June 18–21, 2012. LLNL-ABS-520772.
13. Pascall, A. J., et al., 2011. *Functionally graded, nanostructured materials via patterned electrophoretic deposition*. 4th Intl. Conf. Electrophoretic Deposition (EPD 2011), Puerto Vallarta, Mexico, Oct. 2–7, 2011. LLNL-PRES-500471.
14. Pascall, A. J., et al., 2012. *Modeling the transport of colloids to electrode strips during electrophoretic deposition*. 65th Ann. Mtg. APS Division of Fluid Mechanics, San Diego, CA, Nov. 18–20, 2012. LLNL-ABS-567973

15 Pascall, A. J., et al., 2012. *The fabrication of patterned materials via electrophoretic deposition on dynamic light-actuated electrodes*. 2012 Spring MRS Mtg., San Francisco, CA, April 9–13, 2012. LLNL-POST-544052.

16. Sullivan, K. T., J. D. Kuntz , and A. E. Gash, 2012. "Electrophoretic deposition and mechanistic studies of nano-Al/CuO thermites." *J. Appl. Phys*. **112**, 024316. LLNL-JRNL-550831.
17. Sullivan, K. T., J. D. Kuntz, and A. E. Gash, 2012. *Fine patterning of thermites for mechanistic studies and microenergetic applications*. 9th Intl. Symp. Special Topics in Propulsion, Québec City, Canada, July 9–13, 2012. LLNL-PRES-563776.
18. Sullivan, K. T., et al., 2011. *Directed assembly of energetic materials with micro-engineered architectures*. 2011 MRS Fall Mtg. and Exhibit, Boston, MA, Nov. 28–Dec. 2, 2011. LLNL-POST-516073.
19. Sullivan, K. T., et al., 2012. "Electrophoretic deposition of binary energetic composites." *Combust. Flame*. **159**(6), 2210. LLNL-JRNL-537551.

20. Sullivan, K. T., et al., 2011. *Electrophoretic deposition of binary energetic thermites*. 2011 MRS Fall Mtg. and Exhibit, Boston, MA, Nov. 28–Dec. 2, 2011. LLNL-PRES-516074.
21. Sullivan, K. T., et al., 2012. "Electrophoretic deposition of thermites onto micro-engineered electrodes prepared by direct-ink writing." *J. Phys. Chem. B*, **117**(6), 1686. LLNL-JRNL-560438-DRAFT.
22. Sullivan, K. T., et al., 2012. *Synthesis and reaction mechanism of micro-engineered thermites*. 2012 MRS Fall Mtg. and Exhibit, Boston, MA, Nov. 25–30, 2012. LLNL-PRES-602752.
23. Worsley, M. A., et al., 2011. *Patterned electrophoretic deposition: A bottom-up approach to functionally graded materials*. 2011 MRS Fall Mtg., Boston, MA, Nov. 28–Dec. 2, 2011. LLNL-POST-516711.
24. Worsley, M. A., et al., 2012. *Electrophoretic deposition: A bottom-up approach to functional nanocomposite films*. 2012 Spring MRS Mtg. and Exhibit, San Francisco, CA, April 9–13, 2012. LLNL-PRES-589153.
25. Zheng, X., et al., 2012. "Design and optimization of an LED projection micro-stereolithography manufacturing system." *Rev. Sci. Instrum*. **83**(12), 125001. LLNL-JRNL-575473-DRAFT.
26. Zheng, X., et al., 2012. *Fast, flexible, additive fabrication of complex three-dimensional structures with micro-scale architectures using projection microstereolithography*. 2012 Spring MRS Mtg. and Exhibit, San Francisco, CA, April 9–13, 2012. LLNL-POST-547331-DRAFT.
27. Zhu, C., et al., 2012. *Direct-write assembly of 3D functional materials*. 2011 MRS Fall Mtg. and Exhibit, Boston, MA, Nov. 28–Dec. 2, 2011. LLNL-POST-514973.

Microfluidic Platforms

Elizabeth K. Wheeler

Project Overview

This project focused on modifying existing microfluidic platforms for new applications, including on-chip viral filtration for a viral culturing system and forensic challenge samples for microfluidic sample preparation modules. Ideally, viral culturing would be performed on microfluidic chips to better control cell growth conditions and the introduction of selective pressures in a highly controlled manner. For this to work, the system needs to store produced viruses locally on-chip as they emerge from infected cells, because the viral infection can last as long as a week and cells need a constant infusion of nutrients and removal of waste. To achieve this, we developed a mechanism capable of filtering viruses on-chip while removing accumulated waste products. This work is a continuation of the characterization and evaluation of the integrated microfluidic viral filter.

Previous internal Laboratory funding established microfluidic sample preparation modules that were designed to separate and concentrate emerging pathogens. Their novelty was that the unknown could be isolated—no species-specific tags were used in the separations. This work focuses on applying these same methods to forensic samples, such as buccal (cheek) cells in dirty samples.

We have extensive experience developing microfluidic devices made from multilayer stacks of polydimethylsiloxane (PDMS) containing both fluidic and control microchannels. Each additional layer is stacked and bonded to previous layers. In this project, we worked to integrate porous membrane filters into our existing process. We first established a method to bond our membranes between two PDMS layers, without delaminating, while they are exposed to greater-than-expected fluidic pressures. Next, we sought to evaluate the membrane's efficiency at filtering viruses.

By testing the microfluidic sample preparation modules with forensic samples, we sought to establish this capability within a biosafety level 2 laboratory and evaluate the efficiency of isolating human DNA from complex forensic samples.

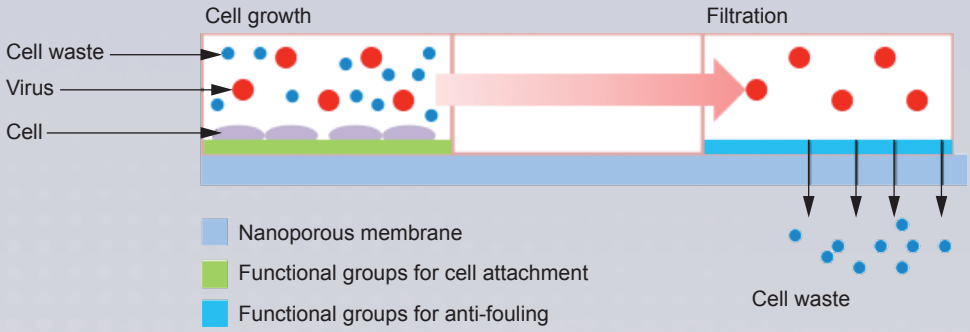

Figure 1. Schematic of multifunctional membrane incorporating a microfluidic viral filtering system.

Relevance to LLNL Mission

At LLNL, we are leveraging a combination of expertise in biology, computation/modeling, and engineering facilities. This work seeks to extend not only our microfluidic platforms to better deliver on the Laboratory's mission in biosecurity but also our future capabilities for viral and other host/pathogen studies.

FY2012 Accomplishments

The system requires the application of multiple surface functionalizations in different locations on a chip as well as efficient viral separation function to achieve high viral concentration (Figure 1). The chip needs to promote adhesion for the cells to form into confluent layers and remain adherent over the experiment. At the same time, the chip needs to contain anti-fouling functionality to separate viral particles from cell waste. Without adhesion layers, cells will form into large, random clumps and will float around, and without anti-fouling coatings, the viruses will rapidly clog pores of the membrane filter and the viral filtration will stop.

By incorporating a multifunctional membrane into the microfluidic device using a stamping method, we succeeded in fabricating a prototype device. The collagen-coated membrane showed good adhesion properties for the cells (Figure 2). The viral filtering device demonstrated high viral filtering efficiencies using an integrated poly(ethylene glycol) methacrylate (PEGMA) functionalized membrane. The track-etched membranes were coated with PEGMA to prevent fouling of the membrane. Different PEGMA grafting methods were evaluated to balance the trade-offs between filtering efficiency and water flux. Filter efficiencies were determined using dengue virus with real-time polymerase chain reaction (PCR) analysis. The use of a surface-initiated atom transfer radical polymerization technique on a PET membrane with 100-nm through-holes resulted in a viral filter efficiency of 99% with a water flux of 40 LMH/bar.

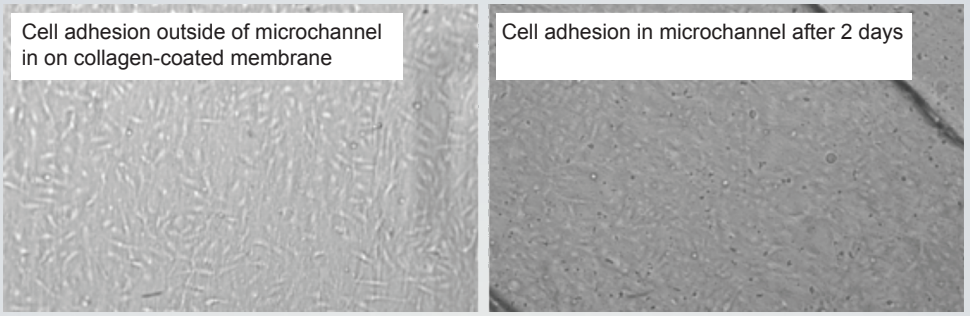

Figure 2. Cell adhesion on collagen-coated membrane surface.

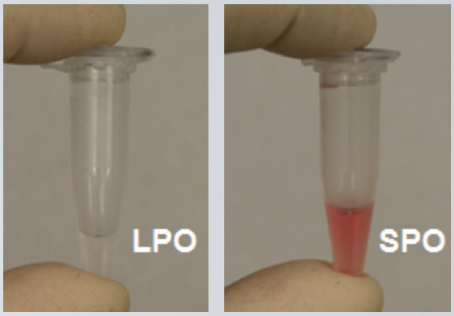

Figure 3: Photos of the output fractions from the acoustic module after processing a blood sample. The bulk of red cells are visually apparent in the SPO.

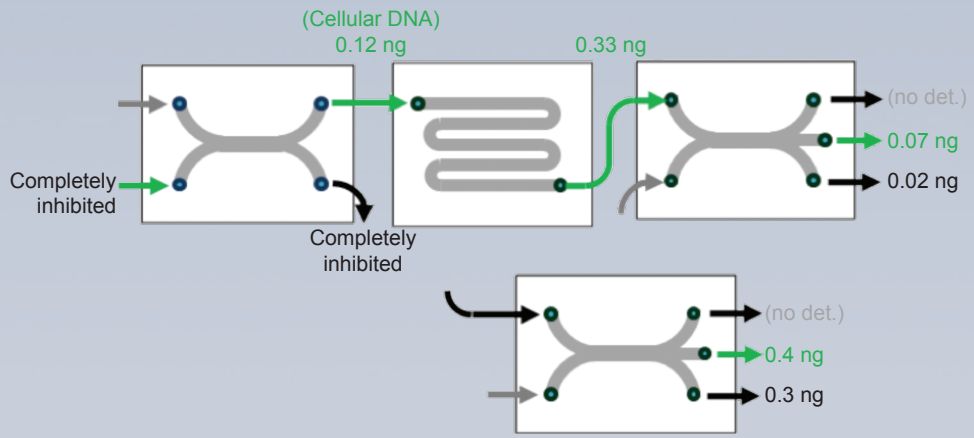

Figure 4: A summary of processing touch samples spiked with humic acid, a PCR-inhibiting compound. A sample that does not initially amplify by PCR is made detectable in two ways: by extraction of cells from an inhibitory mixture in the AF device, or by purification of DNA from an inhibited sample by the ITP module.

Human genomic DNA was successfully extracted from a forensic challenge sample using the acoustic, lysis, and isotachophoresis (ITP) sample preparation modules. The acoustic module separated the buccal cells from other debris in the sample. Subsequent processing in the thermal lysis module opened the cells to "free" the human DNA. Concentration and purification of the DNA from cellular debris occurred in the ITP module. DNA was extracted from buccal cells spiked in sample matrices that contained known PCR inhibitors such as humic acid, commonly in dirt, as well as from touch samples (latent fingerprints).

Related References

1. S. Satyanarayana, R.N. Karnik, and A. Majumdar, "Stamp-and-Stick Room-Temperature Bonding Technique for Microdevices," *Journal Of Microelectromechanical Systems*, 14, 392–399, 2005.
2. K. Aran, L.A. Sasso, N. Kamdar and J.D. Zahn, "Irreversible, direct bonding of nanoporous polymer membranes to PDMS or glass microdevices," *Lab on a Chip*, 10, 548–552, 2010.
3. F. Niklaus, G. Stemme, J.Q. Lu, R.J. Gutmann, "Adhesive Wafer Bonding," *Journal Of Applied Physics*, 99, 2006.
4. B. Chueh, D. Huh, C.R. Kyrtsos, T. Houssin, N. Futai, and S. Takayama, "Leakage-Free Bonding of Porous Membranes into Layered Microfluidic Array Systems," *Anal. Chem.*, 79, 3504–3508, 2007.

Charles Divin

AlignCT: Fine Alignment for X-ray Computed Tomography Systems

Project Overview

The AlignCT project has established a protocol for aligning x-ray computed tomography (CT) systems, combining high-precision radiography phantoms and software alignment algorithms.

Project Goals

It is essential for x-ray CT systems to know the exact trajectory of every ray as it passes through the object. Small misalignments or incorrect distances can quickly degrade the reconstructed contrast and resolution. To operate at peak performance, CT systems undergo a manually intensive periodic alignment process, which relies on measuring the external distances between components. This process is time intensive and relies heavily on radiographer expertise and system-dependent proprietary information.

An improved process needs to be able to determine both the general system geometry, shown in Figure 1, and any misalignments in the detector panel, alignment phantom, and x-ray source. This requires computing the relative location and orientation of the panel and tomography stage, which includes 12 parameters.

Relevance to Lab Mission

X-ray CT provides critical characterization and validation for multiple Strategic Focus Areas. Improving the accuracy of existing systems advances the ST&E Materials on

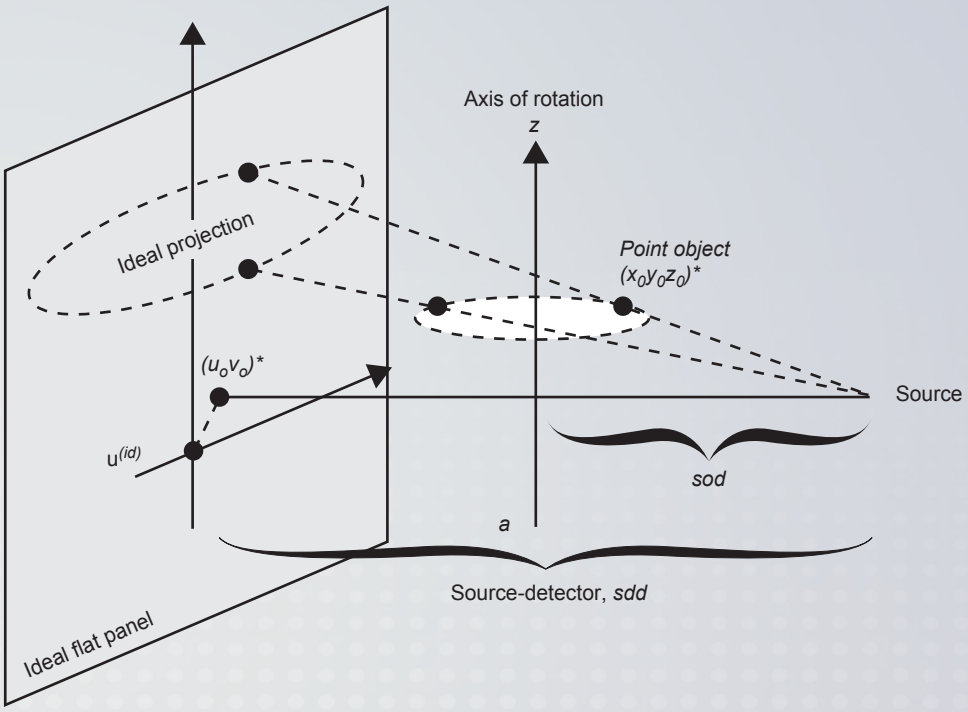

Figure 1. The experimental setup for the perfectly aligned x-ray computed tomography system assumed by CT reconstruction algorithms. The central ray extends from the source and intersects the rotation axis at right angles. If the panel is not perpendicular to the central ray, then the measured projection of a point will differ from the expected, which degrades the reconstruction resolution and contrast.

Figure 2. The left panel shows the alignment radiography phantom. The right panel shows a single x-ray projection from the dataset. The vertical column of steel balls is visible in the center of the phantom.

Demand roadmap goal by providing better data for the validation of predictive modeling and more accurate characterization of engineered or synthesized materials. The project also supports Engineering's core competencies in nondestructive characterization and signal/image processing and control.

FY2012 Accomplishments

Major accomplishments for the project include the fabrication of precision phantoms; the implementation, testing, and validation of alignment algorithms; and the development of a protocol for testing, correcting, and tracking the alignment of our x-ray CT systems.

The design of our alignment phantom is based on a customized version of existing radiography phantoms [1-3]. The easily fabricated design consists of a cylindrical Plexiglas shell embedded with a column of stainless steel balls, as shown in Figure 2. To accommodate different length scales, two phantoms were used: a larger 10-cm phantom with 1-mm balls and a smaller 1-m phantom with 100-µm balls.

The software analysis package consists of two modules written in Matlab: a tracking routine that locates the ball centroids in each projection, and a geometry estimation routine that can work with an arbitrary object distribution. The tracking routine was tested under various contrast and misalignment scenarios, and it was able to successfully trace the orbit of each ball in the presence of moderate misalignments (<5°). Initial system geometry is estimated from the parallax-induced elliptical orbits observed in Figure 3. This estimate is refined by fitting the forward model for a misaligned system to the observed data, after which corrective instructions are displayed for the radiographer.

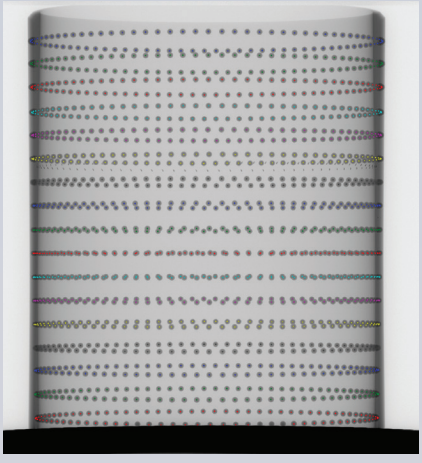

Figure 3. Blend of 90 projections acquired over 360°. The centroid of each ball has been marked by the alignment software.

A graphical user interface was constructed for the Matlab functions and compiled as a stand-alone executable. Figure 4 shows a comparison between a manual alignment and two iterations using the phantom-based alignment.

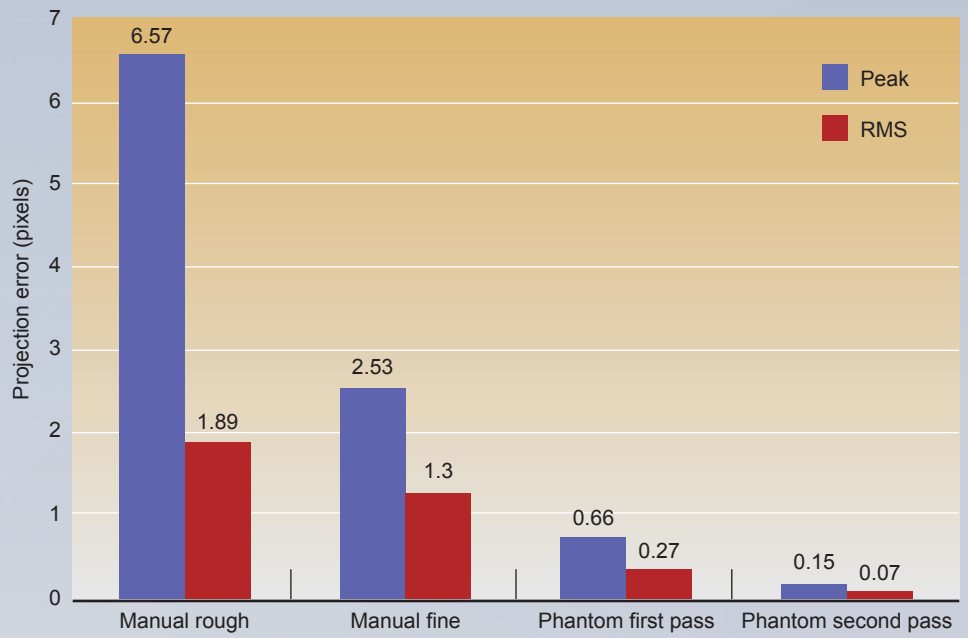

Figure 4. The measured alignment error after each stage. The error measures the distance between a ball centroid in the misaligned coordinates and in ideal coordinates assuming no panel misalignments.

The previous time-intensive manual alignment process was able to level the panel to within 0.04°, adjust the up–down tilt to within 1.0°, and adjust the left–right slant to within 1.5°. With the phantom, these misalignments were reduced to 0.003°, 0.006°, and 0.08°, respectively. This reduced the peak error from 6.5 pixels to 0.15 pixels. For an object near the edges of the CT volume, this reduces the misalignment-induced blurring from 3 pixels to <0.1 pixel.

Related References

1. Chetley Ford, J., D. Zheng, and J.F. Williamson, "Estimation of CT cone-beam geometry using a novel method insensitive to phantom fabrication inaccuracy: Implications for isocenter localization accuracy," *Medical Physics* 38, 2829, 2011.
2. Noo, F., R. Clackdoyle, and C. Mennessier, "Analytic method based on identification of ellipse parameters for scanner calibration in cone-beam tomography," *Phys. Med. Biol.* **45**(11), 3489, 2000.
3. Mennessier, C., Clackdoyle, R., and Noo, F., "Direct determination of geometric alignment parameters for cone-beam scanners," *Phys. Med. Biol.* 54, 1633–60, 2009.

New Capability for Micro- and Nano-scale X-ray Digital Radiography and Computed Tomography

John Sain

Project Overview

In 2011, the LLNL Center for Non-Destructive Characterization procured an Xradia UltraXRM-L200 system to be able to perform nanometer-scale, three-dimensional (3D) x-ray computed tomography (CT) in a standard laboratory environment. The system is the first laboratory-based 3D x-ray microscope at LLNL to offer ultrahigh spatial resolution. It leverages precision x-ray focusing optics and Zernike phase-contrast imaging to deliver volumetric information otherwise only achievable through destructive techniques like cross-sectioning. It provides nondestructive imaging with potentially 50-nm spatial resolution and allows visualization and dimensioning of voids, defects, porosity, and particle distribution. The Non-Destructive Evaluation Group explored its capabilities while characterizing samples for several programs.

The new system provides three immediate benefits: a significant expansion of nondestructive x-ray imaging capabilities with respect to spatial resolution, an on-site location eliminating the potential need to utilize an off-site synchrotron-type facility, and a capability for high-spatial-resolution radiography of classified and unclassified objects.

Project Goals

Our goals were to characterize the as-delivered system performance, explore methods of expanding the stated imaging capabilities, explore strengths and limitations of the x-ray technology, apply algorithms to optimize the x-ray imaging capability, and deliver a procedure for data, collected using proprietary vendor software, to be exported for processing by LLNL software.

Relevance to LLNL Mission

LLNL's recent Five-Year Roadmap to the Future specifies a site-based capability for nanometer-scale x-ray CT. The Xradia system provides this state-of-the-art capability, which benefits multiple programmatic efforts. This new capability helps LLNL maintain its position as a leader in digital radiography (DR) and CT and supports Engineering's core competencies in nondestructive characterization and signal and image processing.

Anticipated programmatic applications of this capability include:

- Inspection of explosives and components by Weapons and Complex Infrastructure.
- Inspection of inertial confinement fusion/high-energy-density target components and experimental refinement of physics-based theoretical models by the National Ignition Facility.
- Detection and imaging of nanoparticles inside tissues for nanotoxicology, characterization of micro- and nanostructures for nanoscience applications, and characterization of material properties by Physical and Life Sciences.
- Characterization of additive-manufacturing microstructures by the Center for Micro- and Nano-technology.

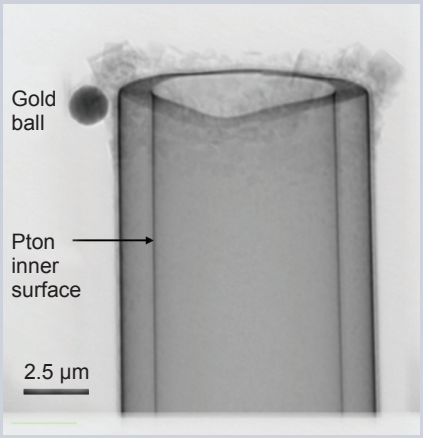

Figure 1. Digital radiograph of the tip of a micropipette that underwent ALD with Pt. The inner surface of the micropipette is coated with a thin layer of Pt estimated to be about 25 nm thick. The micropipette has an outer diameter of 10.3 µm and a wall thickness of 1.3 µm. A small amount of foreign material is stuck to the tip, and a 1.5-µm-diameter gold ball, placed in the field of view as a fiducial, is on the left-hand side.

- Materials engineering and characterization in general, synchrotron-level spatial resolution crucial to in situ, and "4D" studies of microstructural evolution, enabling "materials by design" and other breakthrough research.

FY2012 Accomplishments and Results

We collected CT data for many samples, including micropipettes with atomic-layer-deposition coatings (Figure 1), pressed-powder secondary high explosives (Figure 2), polymer foams (Figure 3), aerogel foams, metallic foams (Figure 4), and composites (Figure 5). DR data was collected to study system spatial resolution, detector signal noise levels, and sample stability.

Some system features were upgraded or added. Filters were installed to reduce the x-ray energy spectrum and thus potentially enhance data quality. A temperature and relative humidity monitor was installed outside the system enclosure because sample stability may be sensitive to local environmental conditions. A microscope was procured for sample inspection and preparation. Unclassified network access was provided. A vendor software module for mitigating potential errors in CT data alignment was integrated. Finally, a procedure was developed to allow vendor CT data to be processed by LLNL algorithms.

We maintained an active relationship with the vendor. Vendor engineers visited LLNL to discuss system performance issues. LLNL personnel received custom training for specific aspects of system operation.

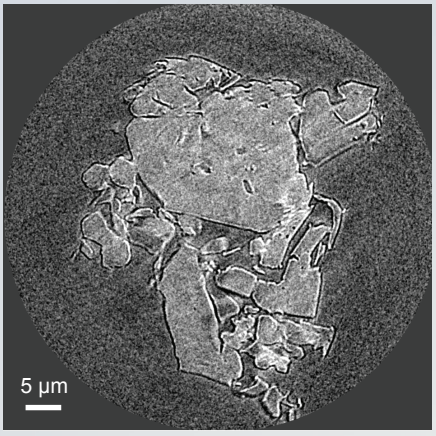

Figure 2. A cross-sectional slice from a reconstructed 3D CT data set of a fragment of a secondary high explosive material. The circular boundary represents the system field of view. The lighter-intensity objects represent particles of explosive material.

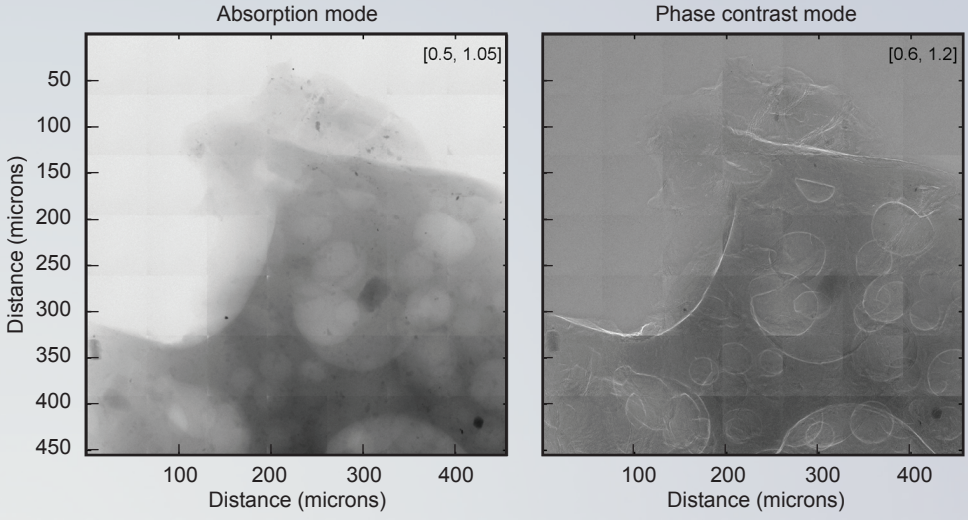

Figure 3. Digital radiographs of an extruded polymer foam containing bubbles of gas and/or air. The absorption-mode image on the left provides a relative measure of x-ray beam attenuation, thus indicating the amount of and/or density of material as a function of position, and the phase-contrast mode image on the right highlights changes in x-ray beam phase, thus enhancing the surfaces and edges in the foam.

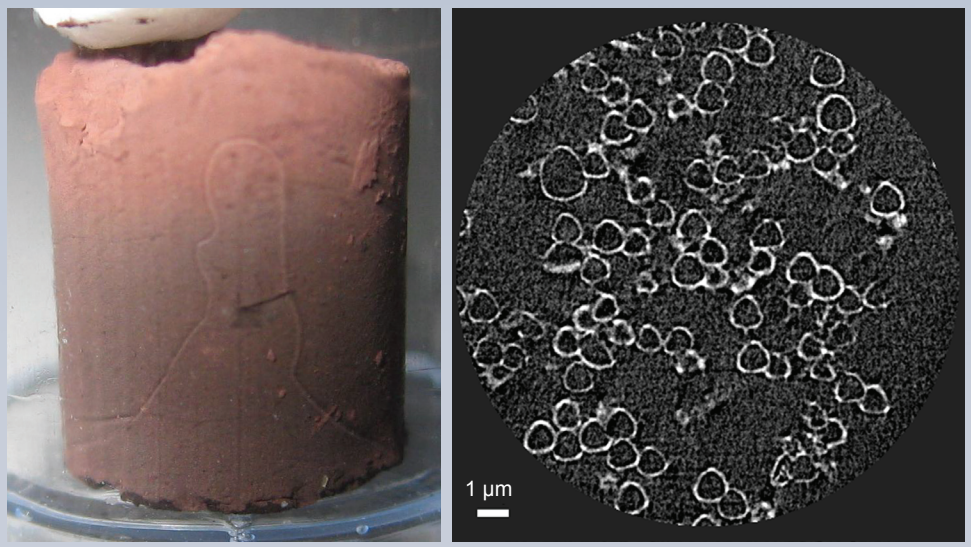

Figure 4. On the left, a cast billet of 10% Cu foam several millimeters in diameter. On the right, a cross-sectional slice of a reconstructed CT data set of a tiny fragment of the copper foam. The clusters of individual hollow "shells" of Cu are easily seen.

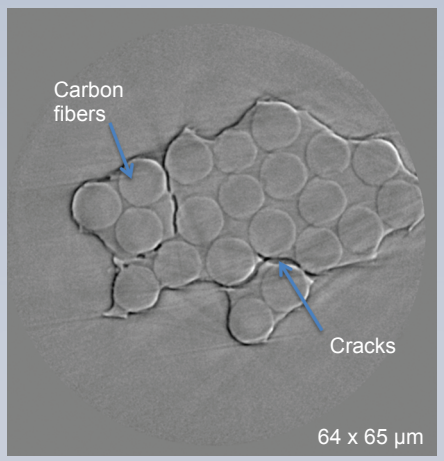

Figure 5. A cross-sectional slice of a phase-contrast CT data set of a bundle of 21 carbon fibers in an epoxy matrix. The cross-section of each fiber is clearly seen, and some cracks between certain groups of fibers have been detected.

Related References

1. Tkachuk, A. et al., "X-ray computed tomography in Zernike phase contrast mode at 8 keV with 50-nm resolution using Cu rotating anode x-ray source," *Z. Kristallogr.*, 222, 650–655, 2007.
2. Feser, M. et al., "Sub-micron resolution CT for failure analysis and process development," *Meas. Sci. Technol.*, 19, 094001, 2008.

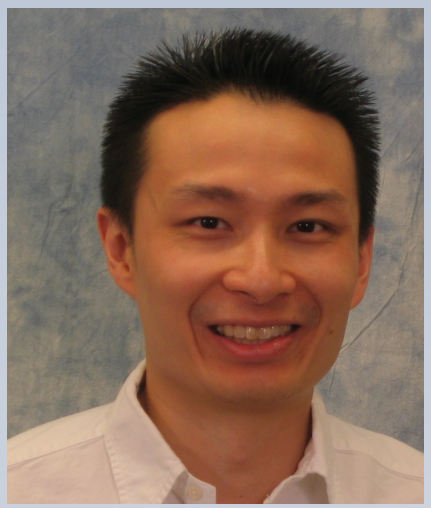

Vincent Tang

Investigation of Fast Z-pinches for Scalable Large-Current High-Gradient Particle Accelerators

Project Overview

Our objective is to study extremely high (MV/cm) acceleration gradients in fast Z-pinch plasmas for next-generation accelerator applications. Empirically, Z-pinch plasmas, such as those produced by technologically simple Dense Plasma Focus (DPF) devices, have emitted ion beams with up to approximately 10-MeV ions over centimeter scales. The mechanisms behind the large acceleration gradients responsible for these ion beams are still not well understood. We will perform unique, first-ever probe–beam experiments to measure the gradients directly and develop state-of-the-art fully kinetic plasma simulations to better understand Z-pinch plasmas and validate a predictive capability.

Our motivation is twofold. First, at the megavolt level, DPF Z-pinch devices optimized for beam production and acceleration could serve as the basis for compact, intense radiological sources—such as directional neutron sources—and also as unique high-current ion injectors. Second, if the acceleration gradients can be scaled to higher levels, our research could lead to very-high-gradient, plasma-driven accelerators notably simpler than current laser or electron-beam systems, thus revolutionizing accelerator technology and applications.

Project Goals

We expect to produce a fundamental understanding of acceleration gradients in DPF Z-pinch plasmas and use that knowledge to examine how these plasmas can be systematically exploited for accelerator applications. Experimentally, we will inject, for the first time, a 200-ps, 4-MeV ion probe beam into a DPF Z-pinch plasma and measure the acceleration of the probe beam to deduce the plasma's acceleration. We will refurbish a 4-MV RFQ for the probe beam and construct

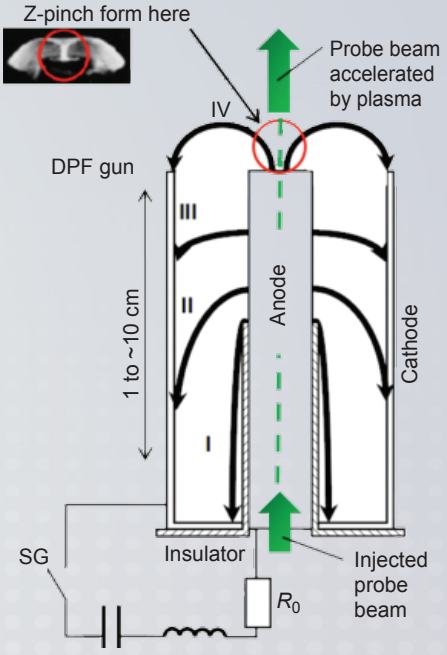

Figure 1. DPF and the proposed probe beam injection experiment. In a DPF, the Z-pinch plasma is formed at the end of a coaxial gun through multiple stages. The annular cathode is typically made up by a series of rods leaving open gaps. First, the plasma sheath starts from flashover of the insulator (I), accelerates axially down the electrode by J x B forces along the coaxial gun (II, III), and collapses radially (IV) to form a dense, fast Z-pinch lasting 10's to 100 ns at the end of the anode with internal electric field gradients exceeding 100 MV/m. The inset shows an image of such a Z-pinch. In our experiment, we will inject a 4-MeV probe beam through a hollow central electrode in the coaxial gun and directly measure, for the first time, the plasma's acceleration gradients at various times during the Z-pinch.

a table-top DPF for the plasma. The unique probe beam data will be compared with the first-ever fully kinetic Particle-in-Cell (PIC) simulation of these Z-pinch plasmas in order to validate useful predictive simulations for applications.

Relevance to LLNL Mission

The work supports LLNL's national security missions—specifically homeland security, nonproliferation, and accelerator science—by providing the technological and scientific basis for compact alternative radiological sources and next-generation accelerator technology for active interrogation and radiography. Successful resolution of the physics behind the Z-pinch plasmas formed in a DPF device would resolve long-standing questions in plasma physics and in High Energy Density Laboratory Physics (HEDLP), both of which are core Livermore competencies.

FY2012 Accomplishments

This past year, we:

- Produced and characterized record sub-kJ and kJ DPF plasmas with ion beam energies of 400 keV and gradients greater than 50 MV/m.
- Assembled the 4-MeV radio-frequency quadrupole ion probe beam and the beam transport required for it, and conducted the first-ever beam-into-DPF plasma experiments (Figure 1).
- Completed first-ever simulations of the DPF through both fully kinetic PIC and hybrid models.
- Began comparison of these leading models results with experimental data, such as neutron yield, with good initial agreement.
- Hired an additional postdoctoral researcher in the area of high-energy-density physics.

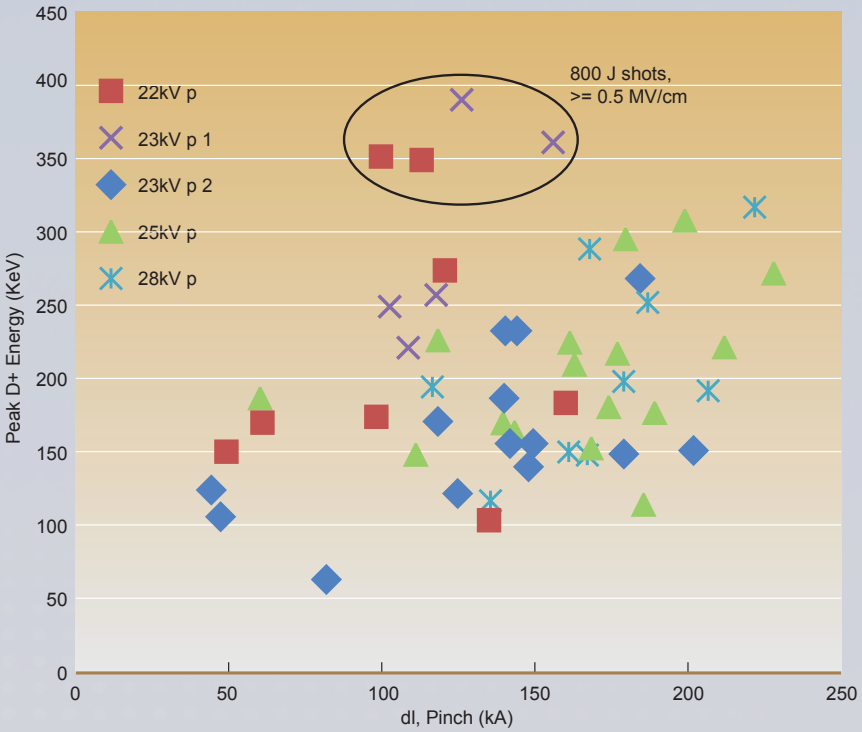

Figure 2. Peak deuteron energy measured from our DPF as a function of pinch current. Record acceleration gradients greater than 0.5 MV/cm were measured for sub-kJ DPF plasmas.

Figure 3. Our table-top DPF gun and a typical pinch plasma. The first fully kinetic simulations of DPF Z-pinch plasmas were successfully completed.

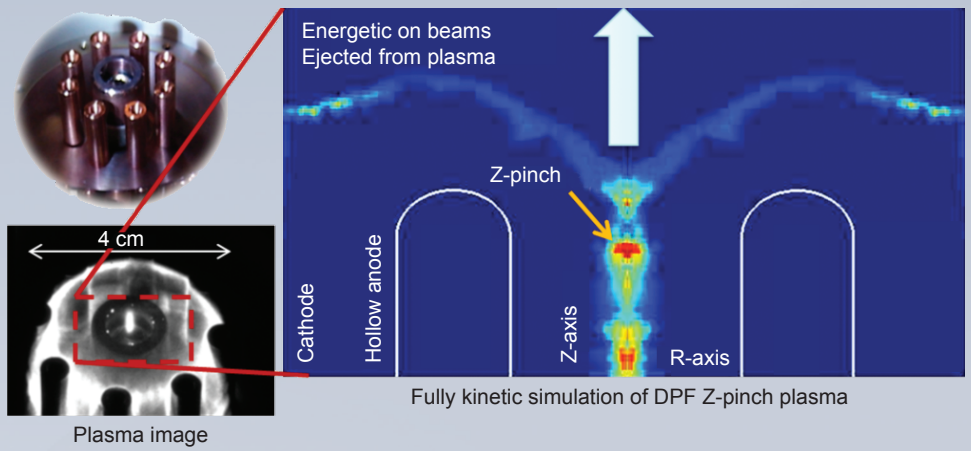

Figure 4. Overview of the probe beam injection experiment showing the RFQ accelerator providing the 4-MeV probe beam, a beam transport section, the DPF, and the Thomson spectrometer for diagnosing the accelerated probe beam.

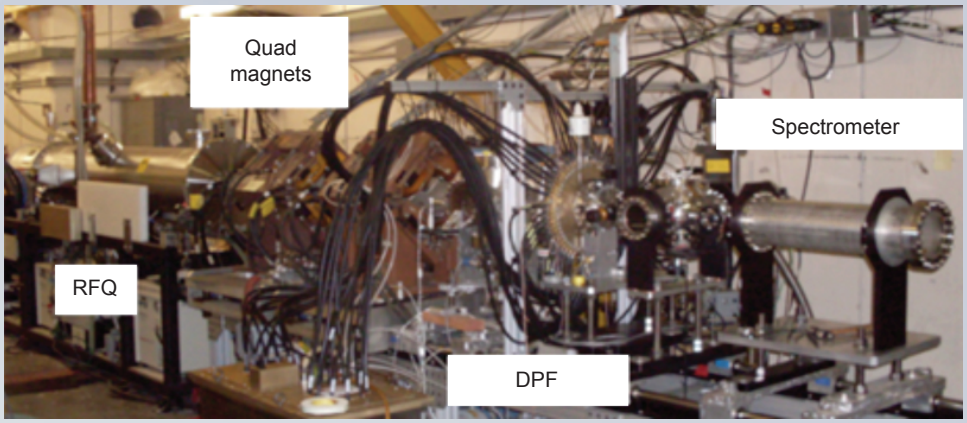

FY2013 Proposed Work

In FY2013, we will (1) continue and complete the first-ever probe–beam experiments and compare results to predictions from our fully kinetic models to produce a new understanding of acceleration mechanisms in DPF devices, (2) determine the viability of using our DPF device as an injector for an induction linear accelerator, and (3) examine the feasibility of staging DPF devices for a next-generation high-gradient accelerator.

Related References

1. V. Tang, M.L. Adams, and B. Rusnak, "Dense Plasma Focus Z-pinches for High Gradient Particle Acceleration," *IEEE Transactions on Plasma Science*, **38**(4), 719–727, 2010.
2. A. Schmidt, V. Tang, and D. Welch, "Fully Kinetic Simulations of Dense Plasma Focus Z-Pinch Devices," *Phys. Rev. Lett.*, 109, 205003, 2012.
3. J.W. Mather, "Investigation of the high-energy acceleration mode in the coaxial gun," *Phys. Fluids Suppl.*, 7:5, 1964.
4. J.W. Mather, "Formation of a High-Density Deuterium Plasma Focus," *Phys. Fluids*, **8**(2):366, 1965.
5. G. Decker and R. Wienecke, "Plasma Focus Devices," *Physica*, 82C:155, 1976.
6. D.D. Ryutov, M.S. Derzon, and M. K. Matzen, "The physics of fast Z pinches," *Rev. Modern Physics*, **72**(1), 167–223, 2000.

Ultrafast, Sensitive RadOptic Gamma, Neutron, and Proton Detector Development

Steve Vernon

Project Overview

In this project, we seek to build a novel class of radiation detectors that leverage recent advances in the development of high-bandwidth x-ray-to-optical converters and high-bandwidth optical recording technologies with enhanced sensitivity and temporal response. The new class of detectors will support future high-energy-density (HED), Weapons and Complex Integration (WCI), and inertial confinement fusion (ICF) experiments at the National Ignition Facility (NIF) [1-4].

Project Goals

The goal is a new class of gamma (γ), neutron (n), and proton (p) detection systems with response times in the picosecond range. Our concept uses conversion of the incident radiation to secondary electrons, which interact with a RadOptic semiconductor sensor and generate a non-equilibrium charge distribution. An optical "replica" of the initial radiation signature is produced by interrogating the RadOptic sensor with an optical probe beam. Each of the detection systems incorporates unique radiation to secondary charged particle (electron) converters, RadOptic sensors, and state-of-the-art high-bandwidth optical recorders.

The design of the converters is the primary deliverable of the project. The n converters are relatively simple and rely on secondary electron generation in a CsI photocathode by interaction of a recoil p or deuteron (d) generated in an inelastic collision between the incident n and nuclei in a plastic foil. The γ converter is significantly more complicated in its design and employs a combination of pair production, Cherenkov radiation, and secondary electron generation in CsI. Both implementations rely on electron optics to increase the beam intensity at the RadOptic sensor. The project is focusing on predictive simulation of converter performance, using MCNP and GEANT codes, to optimize converter architecture.

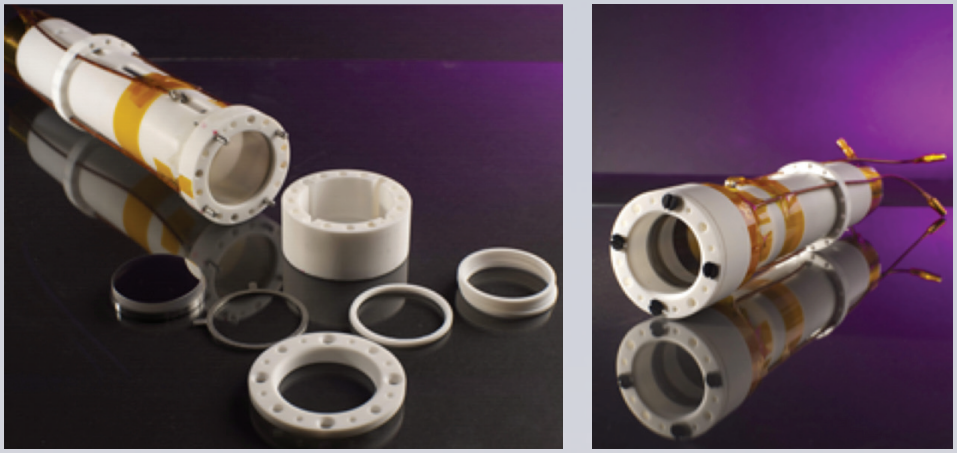

Figure 1. (left) Exploded view and (right) assembled laser photocathode and electron optics system.

The back-end recorder of the detection system incorporates recently developed and demonstrated high-bandwidth, RadOptic semiconductor sensors and ultrafast, all-optical recorders [5]. Initial testing of sensors will be accomplished using high-bandwidth photodiode detectors and oscilloscopes as the data recording systems.

Relevance to LLNL Mission

The project is well aligned with LLNL's institutional science and technology plan. The detection systems being developed address programmatic needs for three-dimensional, time-resolved validation of experimental results in support of HED, WCI, and ICF experiments at NIF. The research is undertaken within the Measurement and Experimental Sciences S&T Pillar supporting the Stockpile Stewardship Focus Area.

FY2012 Accomplishments

Major accomplishments included:

- Design of optimized Fabry-Perot and Gires Tournois InGaAsP electron sensors.
- Modeling of the spatial and temporal distribution of the electron cascade produced by radiation absorption in GaA.
- MCNP and GEANT modeling of the *γ* and *n* converters.
- Demonstration of the electron source: an intense, pulsed, electron source comprised of a back-side illuminated Au photocathode excited by a frequency tripled, ~200-fsec pulse width, Ti:sapphire laser.
- Design, fabrication, and implementation of the electron optics system to produce a demagnified, 20-keV electron image of the photocathode at the RadOptic sensor and preserving the temporal distribution of the emitted electrons.

We have also developed a robust method for aligning, fiber-coupling, and packaging the RadOptic sensor that admits actinic metrology (1550 nm) of the sensors during fabrication and allows tailoring of the optical response during the fabrication process, increasing sensor performance and process yield.

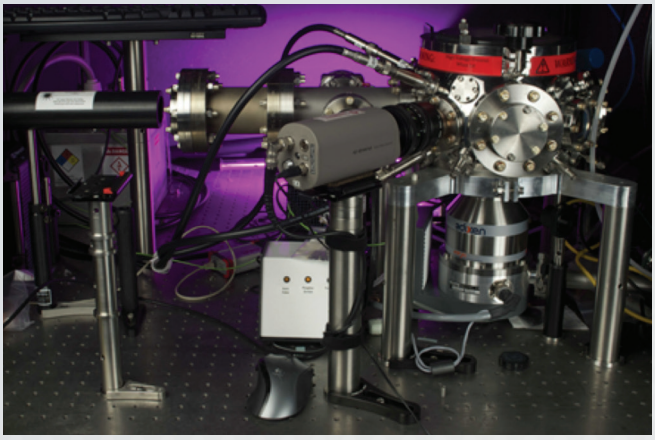

Figure 2. UHV electron optics and sensor test system.

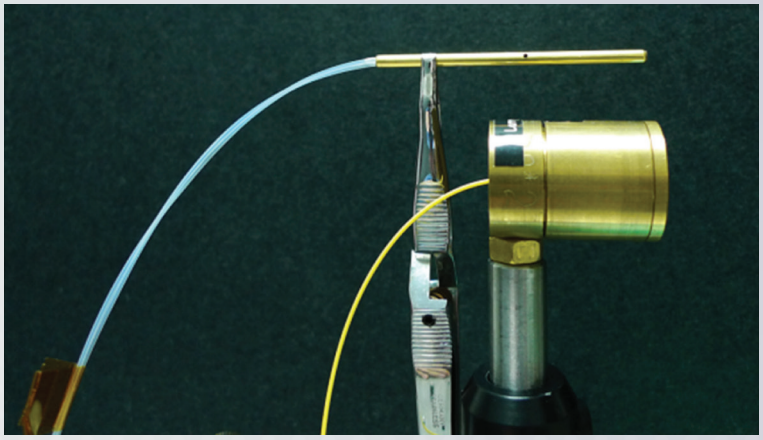

Figure 3. New, miniaturized (φ = 180 μm) dual-fiber RadSensor package compared to original design.

FY2013 Proposed Work

In FY2013 we will fabricate optimized RadOptic sensors; integrate the optimized sensors, electron optics system, and TimeLens recorder; and demonstrate ultrafast RadOptic electron detection. We will complete the simulation-based design of the *n* and *γ* converters using a combination of MCNPX and GEANT codes to optimize converter efficiency and temporal response.

Related References

1. M.E. Lowry, et. al., *Proc. SPIE* 5194, 193–204, 2004.
2. M.E. Lowry, et. al., *Rev. Sci. Instr.* 75, 3995-3997, 2004.
3. B. Ziaja, et. al., *J. Appl. Phys.* 97, 064905, 2005.
4. M.E. Lowry, et. al., *Ultra Fast Optics*, Monterey, CA, 2011.
5. S.P. Vernon, et. al., *Rev. Sci., Instrum.* 83, 10D307, 2012.

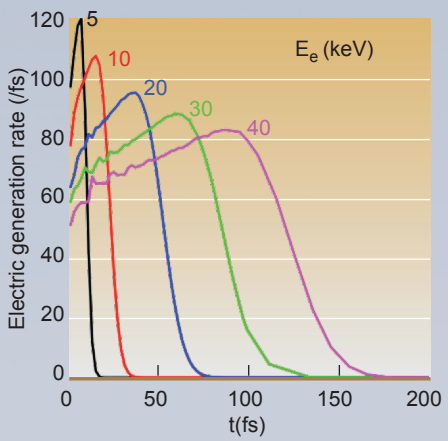

Figure 4. Simulation of the electron generation rate for incident electrons of 5, 10, 20 , 30, and 40 keV in GaAs. The simulations indicate that the refractive index change (which is proportional to the generated charge) occurs on a sub-ps timescale.

LLNL-TR-657598